Translational Oncology

www.transonc.com

Volume 4 Number 6 December 2011 pp. 377–389 377

Chaperon-like Activation of Serum-Inducible Tryptophanyl-tRNA Synthetase Phosphorylation through Refolding as a Tool for Analysis of Clinical Samples[1]

Elena L. Paley*,†

*College of Allied Health and Nursing, Nova Southeastern University, Kendall Campus, Miami, FL, USA; †Expert BioMed, Inc, Miami, FL, USA

Abstract

Tryptophanyl-tRNA synthetase (TrpRS) expression alters in colorectal (CRC), pancreatic (PC), and cervical (CC) cancers. Here, phosphorylation of unfolded TrpRS and its fragments is stimulated by human cancer sera (CS; $n = 13$) and serum of rabbit tumor induced by Rous sarcoma virus, unaffected by donor sera (NS; 11/15) and abolished by alkaline phosphatase. At 20 years of follow-up, serum-inducible TrpRS phosphorylation found years before healthy donors (3/15) diagnosed with PC, CRC, or leukemia. I have examined a specificity of serum-inducible TrpRS phosphorylation and found, surprisingly, that serine phosphorylation of unfolded TrpRS is stimulated by anti-TrpRS rabbit antisera but is unaffected by rabbit nonimmune sera and antisera to other antigens. Anti-TrpRS immunoglobulin G (IgG) inhibits phosphorylation of full-length TrpRS and stimulates phosphorylation of its 20-kDa fragment. Phosphorylation of this fragment is stimulated also by CS but not NS. 2-Mercaptoethanol and cyclic AMP exerted synergistic inhibitory effect on TrpRS phosphorylation. Anti-TrpRS sera and casein act as chaperones increasing TrpRS phosphorylation through refolding. Histone-specific protein kinase activity in CS ($n = 44$) and anti-TrpRS sera was lower than that in NS ($n = 11$), rabbit nonimmune sera and antisera to other antigens. TrpRS inhibitors, tryptamine, and tryptophanol stimulate *in vivo* accumulation of enzymatically inactive, nonphosphorylated, aggregated and anti-TrpRS IgG refoldable TrpRS. Phosphorylation of postsurgical tissues ($n = 18$) reveals TrpRS in ovarian cancer (OVC) and CC but not in normal placenta and liver. In OVC, TrpRS phosphorylation increase correlates with elevated tryptophan-dependent ATP–inorganic pyrophosphate exchange. Although not inducing cancer, TrpRS triggers signaling concomitant with cancer.

Translational Oncology (2011) 4, 377–389

Introduction

Some malignancies, notably lung cancer and pancreatic cancer (PC), are mostly detected only in late stages. Screening tests of bodily fluids are a way of detecting cancer early, before there are any symptoms. Tryptophanyl-tRNA synthetase (TrpRS) catalyzing attachment of its substrate, tryptophan, to cognate $tRNA^{trp}$ in protein biosynthesis is suggested to be a prognostic marker in cancer tissues [1–4]. TrpRS belongs to a family of aminoacyl-tRNA synthetases (ARS). The first step in ARS activity is amino acid activation with formation of aminoacyl-adenylate and release of inorganic pyrophosphate (ATP-PP_i exchange), and the second step is formation of aminoacyl-tRNA. In colorectal cancer (CRC), changes in TrpRS expression correlate with survival: a low protein expression in human tissues correlated with a worse cancer prognosis (increased risk for recurrence and worse survival) than a higher human TrpRS (hTrpRS) expression [1]. In human pancreatic cancer (PC) cells, high messenger RNA (mRNA) and protein TrpRS expression correlates with higher growth rate and metastatic ability, whereas hypoxic state associates with reduced hTrpRS expression. Inversely, the alternatively spliced antiangiogenic TrpRS-truncated form

Address all correspondence to: Elena L. Paley, PhD, 1301 NE Miami Gardens Dr, Miami, FL 33179. E-mail: ep180@nova.edu; elena_paley@bellsouth.net

[1]This article refers to supplementary materials, which are designated by Tables W1 to W7 and Figures W1 to W6 and are available online at www.transonc.com.

Received 11 July 2011; Revised 11 July 2011; Accepted 22 August 2011

1944-7124/11/ DOI 10.1593/tlo.11220

is upregulated by hypoxia. Therefore, alternatively spliced TrpRS forms are differentially regulated by hypoxia in PC cells [3]. Tumor hypoxia is associated with higher metastatic ability and worse prognosis. TrpRS is identified as a marker in cervical cancer (CC) that originates from human papillomavirus infection and progresses through histologically defined premalignant stages. TrpRS protein expression has been compared in normal cervical epithelium and patient-matched high-grade squamous intraepithelial lesions (HSIL) with cervical carcinoma tissue from the same patient population [2]. An increase in TrpRS expression (1.7-fold) was found in cervical carcinoma compared with that in normal tissue. TrpRS expression was decreased (1.4-fold) in HSIL compared with that in normal and was upregulated (2.4-fold) in cancer compared with that in HSIL [2]. TrpRS protein is upregulated (2.7 times) in clear cell adenocarcinoma, with a highly malignant potential in human epithelial ovarian cancer (OVC) when compared with mucinous ovarian adenocarcinoma of low malignant potential [4]. TrpRS gene expression is upregulated 5.7-fold by ovarian hormone estrogen [5], which is able to promote cell proliferation in the breast and the uterus.

TrpRS is an interferon-inducible protein upregulated in hosts after some viral infections. TrpRS gene expression is induced in the liver during hepatitis B viral clearance [6] and upregulated (1.65-fold) by the K15 protein of Kaposi sarcoma–associated herpesvirus [7]. Notably, TrpRS mRNA expression is upregulated 800-fold at 8 hours after infection with human cytomegalovirus [8], a frequent opportunistic infection in immunocompromised individuals particularly those receiving organ transplants and harboring human immunodeficiency virus infection.

$tRNA^{trp}$ used to prime reverse transcription in Rous sarcoma retrovirus (RSV). TrpRS is present in RSV at approximately 12 molecules/virion, but the determined number of avian TrpRS molecules in RSV may be an underestimate [9]. The product of RSV is a transforming phosphoprotein pp60 src. Recent studies have shown that c-src, a nonreceptor tyrosine kinase, exhibits elevated protein levels and activity in numerous types of human cancers [10]. Furthermore, it has been found to be a critical component of multiple signaling pathways that regulate proliferation, survival, metastasis, and angiogenesis [11]. The role of retrovirus-specific packaging of TrpRS is not known.

Bovine TrpRS (bTrpRS) is a serine/threonine phosphoprotein. The 60-kDa bTrpRS and its 40-kDa proteolytic forms exhibit similar phosphopeptides [12]. Protein kinase (PK) associated with bTrpRS (TrpRS-PK) phosphorylates nuclear protein histones, preferably histone H2B [12]. TrpRS-PK, with molecular mass ~60 kDa (under denaturing conditions), is copurified and coimmunoprecipitated with TrpRS. Protein phosphorylation is one of the most significant signal transduction mechanisms by which intercellular signals regulate crucial intracellular processes such as ion transport, cellular proliferation, and hormone responses [13]. Consistent with the complex role of this posttranslational modification in the cell, phosphorylation can be regulated by activators or inhibitors and phosphorylation can be regulated by other proteins or by themselves (autophosphorylation). TrpRS binds to its substrate, tryptophan, whereas increase in plasma-free tryptophan concentrations is a common feature of both human solid and hematologic malignancies and some experimental tumors [14–18]. Amino acids stimulate ribosomal protein S6 phosphorylation [19]. TrpRS *in vivo* phosphorylation is modulated in bovine kidney (MDBK) cells [20] and human CC (HeLa) cells [21] by tryptophan analog, tryptamine—a TrpRS competitive inhibitor. Tryptamine is a metabolic product of tryptophan decarboxylation by aromatic L-amino acids decarboxylase. Abnormally aggregated TrpRS was found in tryptamine-treated cells and in a brain of a patient with Alzheimer disease (AD) [22–24]. Anti-TrpRS monoclonal antibody is able to disaggregate the self-assembled fibrils of TrpRS-derived NH_2 peptide [23]. TrpRS protein expression but not mRNA expression is downregulated by wild-type p53, a tumor suppressor, suggesting binding of p53 and TrpRS [25]. The p53 accumulates in response to cellular stress, e.g., DNA damage, oncogene activation, and hypoxia. TrpRS is tightly associated with DNA polymerase α [26]. Heme, a porphyrin coordinated with Fe, binds hTrpRS and regulates its tRNA aminoacylation activity [27]. Porphyrins have been increased in the blood of individuals with different tumor types [28]. The specific function of TrpRS phosphorylation has not yet been identified. For some other ARS, phosphorylation may affect the enzymatic activity [29]. In this study, TrpRS and histones were used as exogenous substrates to explore serum-inducible phosphorylation in a human cohort and in rabbits including rabbit bearing tumor induced by RSV (TBR). TrpRS as an endogenous substrate in the phosphorylation of human normal tissues and malignant and nonmalignant gynecologic tumors was also studied.

Materials and Methods

Human Tissue and Serum Samples

Postsurgical tissues were provided by Dr Nikolai E. Zinov'ev, MD (N. N. Blokhin Russian Cancer Research Center, Moscow, Russia). Human blood samples were provided by Dr Regina R. B. Paley, MD (City Hospital 15, Tashkent, Uzbekistan), or were obtained from National Oncological Scientific Center, Tashkent, Uzbekistan, and volunteers. Ethical approval (no. 00-001) was obtained from the ethics committee at Expert BioMed, Inc (Miami, FL).

Purification of bTrpRS

bTrpRS was purified from bovine pancreas using two different protocols (A and B) as described previously [12]. Purified bTrpRS was stored (–80°C) in 0.5 mM dithiothreitol (DTT; Sigma, St Louis, MO), 0.1 mM tryptophan, 0.1 mM EDTA, 10 mM Tris-HCl, pH 7.5, and 0.7 mM di-isopropyl fluorophosphate (DFP) or under 60% ammonium sulfate (Merck, Whitehouse Station, NJ). TrpRS precipitated by ammonium sulfate precipitation TrpRS was dialyzed (3.5 hours) before use against distillated water (90 minutes) and water changed (2 hours) or dialyzed (48 hours) against water (24 hours) and finally against 10 mM Tris-HCl, pH 7.2 (24 hours at 4°C).

Rabbit Antisera, Immunoglobulin G, and Monospecific Polyclonal Antibodies Specific to TrpRS

Rabbits (*Chinchilla* sp) were immunized by four subcutaneous injections with bTrpRS purified using protocol A (5 mg/animal) in Freund adjuvant (Difco, Franklin Lakes, NJ) with intervals of 21 days, 26 days, and 9 months. Blood was collected on the eighth day after the last injection.

To isolate the anti-TrpRS immunoglobulin G (IgG) fraction, 20 ml of borate buffer (0.15 M NaCl, 0.2 M boric acid, pH 8) was added to anti-TrpRS rabbit serum (20 ml). Then, 2.53 M Na_2SO_4 (40 ml) was added for precipitation (1 hour). After centrifugation, pellets were dissolved in 0.15 M NaCl and an equal volume of 2.53 M Na_2SO_4 was added (1 hour, room temperature). After centrifugation, the pellet was resuspended in 0.15 M NaCl (40 ml) and dialyzed against water (1 L for 1 hour), then against 0.15 M NaCl (2 L for 2 hours), and against 0.15 M NaCl (2 L overnight at 4°C); two more changes (1 L each) with 0.1 M sodium phosphate buffer and 0.15 M NaCl, pH 7 (phosphate-buffered saline [PBS]) overnight (4°C), were made. After dialysis, the anti-TrpRS IgG fraction was further purified on

diethylaminoethyl (DEAE) 52-cellulose (column of 9-cm height × 2.2-cm diameter) prewashed with PBS and was eluted (40 ml at 4°C). The protein concentration was 1 mg/ml. To obtain monospecific polyclonal antibodies, 1% aminocellulose was used (kindly provided by Dr R.S. Nezlin). To convert aminocellulose into diazocellulose, hydrochloric acid (0.33 ml of undiluted HCl) was added to aminocellulose (2 ml) and then $NaNO_2$ (45 mg) was added (in ice for 35 minutes). The diazocellulose was washed with borate buffer (60 ml at 4°C) and then incubated with 200 μl of TrpRS (10 mg/ml) in borate buffer (1 ml) overnight at 4°C. The TrpRS-diazocellulose was washed three times with borate buffer and was resuspended in the same buffer (2 ml) with sodium azide (0.02%). The IgG fraction eluted from DEAE 52-cellulose (20 ml) was incubated with TrpRS immobilized on diazocellulose (300 μl; 1.6 mg of TrpRS/ml of diazocellulose) overnight at 4°C. After centrifugation, TrpRS-diazocellulose was washed six times with 0.01 M sodium phosphate buffer and 0.15 M NaCl (100 ml), eluted with 0.2 M glycine-HCl pH 2.5 (350 μl for 15 minutes), neutralized with supernatant (monospecific antibodies; 5 M NaOH), and stored with sodium azide (0.02%). The antibody used here is specific for cytoplasmic TrpRS.

Casein

Total casein was isolated from cow's milk as described [30] and lyophilized (provided by Dr Y.Y. Kit). Casein (10 mg/ml in 0.1 M Tris-HCl pH 8.7 or water) was preboiled for 25 or 5 minutes to inactivate possible PK activity before use. Molecular weights of casein forms are from 23.6 (αs-casein) to ~34 kDa.

Histones

Total histones were isolated from the nuclei of Wistar rat thymus by acid extraction with 0.4 M H_2SO_4 or $HClO_4$ followed by neutralization, dialysis, and purification by chromatography on Amberlite CG-50. Lyophilized histones were kindly provided by Dr Y. S. Mangutova. The histones included subclasses H1/H5 (linker histones) and histone core containing H2A and H2B (doublet), H3 and H4.

Rabbit Polyclonal Antisera Specific for α-Fetoprotein or Thomsen-Friedenreich Antigen

Lyophilized rabbit monospecific antiserum to α-fetoprotein (AFP) was dissolved in water (1 ml). Polyclonal rabbit anti–human AFP is from the diagnostic kit (produced by N.F. Gamaleya Institute for Epidemiology and Microbiology, Moscow, Russia). Affinity-purified AFP from the serum of a patient with hepatocellular carcinoma was used as antigen. Polyclonal rabbit undiluted antiserum against carcinoma-associated Thomsen-Friedenreich (TF) antigen from human breast tissue [31] was provided by Elnora Daminowa (National Oncological Scientific Center, Tashkent, Uzbekistan). Rabbits were immunized twice in lymph nodes by TF.

Multienzyme ARS Complex

Some phosphorylation experiments were conducted with multienzyme complex from rabbit liver (fraction A) containing seven ARS isolated as described [32] and provided by Drs Alexey Wolfson and Valery Filonenko.

Immunoprecipitation of bTrpRS by TBR Serum Followed by Immune Complex PK Activity Testing

Purified bTrpRS (20 μg/sample) was preincubated with nonimmune rabbit serum (2 μl) in PBS (100 μl for 1 hour at 37°C). Then, 10% protein A–*Staphylococcus aureus* in 0.15 M NaCl, 0.01 M sodium phosphate pH 7.2, 1% NP-40 (Sigma), 1% sodium deoxycholate (Sigma), 0.5% SDS, and 3 mM phenylmethylsulfonyl fluoride (PMSF; RIPA buffer) were added (20 μl) for 20 minutes at 37°C. Supernatants were incubated with 2 μl of either nonimmune rabbit sera or TBR serum (kindly provided by Dr N. Mazurenko [10]) overnight at 4°C and then with 10% *S. aureus* (13 μl/probe) for 30 minutes at 37°C. Pellets were washed three times with RIPA buffer (1 ml), once with 10 mM Tris-HCl, pH 7.2, 3 mM PMSF (1 ml), once in 1 ml of 20 mM Tris-HCl (Calbiochem, Basel, Switzerland), pH 7.2, 2 mM $MnCl_2$ (Fluka, La Jolla, CA), 5 mM $MgCl_2$, 1 mM 5′AMP, 50 mM 2-mercaptoethanol (2-ME), 50 μM EDTA, and 3 mM PMSF (PK buffer). Pellets were incubated in PK buffer with the addition of [γ-^{32}P]ATP (1.5 μl/probe, 2000 Ci/mmol, 500 μCi/0.05 ml of water; Institute of Nuclear Physics, Uzbekistan) for 15 minutes at 37°C. PK reaction was terminated by Laemmli sample buffer (4 μl) by boiling for 5 minutes. Supernatants were analyzed on 12.5% SDS–polyacrylamide gel electrophoresis (PAGE). Protein markers used for SDS-PAGE (14-94 kDa; Pharmacia, Uppsala, Sweden) were as follows: phosphorylase B (94 kDa), albumin (67 kDa), ovalbumin (43 kDa), carbonic anhydrase (30 kDa), trypsin inhibitor (20.1 kDa), and α-lactalbumin (14.4 kDa). Gel was stained with Coomassie blue and dried, and autoradiography was obtained.

Tissue Extracts and Immunoblot Analysis

Tissue specimens were cut with scissors in the lysis buffer (0.25 M sucrose [Merck], 0.01 M Tris-HCl pH 7.5, 1 mM DFP at 0°C or in 50 mM Tris-HCl pH 7.5, 50 mM KCl, 1.5 mM EDTA, 10 mM $MgCl_2$, 1 mM DTT, 10% glycerol, and 3 mM DFP) and homogenized in glass/glass homogenizer with a tight-fitting pestle. Mitochondrial fractions were obtained by differential centrifugation. The extracts were spun at 600*g* at 2°C; the supernatant was spun at 12,000*g* at 2°C. The postmitochondrial supernatant was kept frozen at −80°C until use or was used after preparation. To remove cytoplasm from the samples, mitochondrial pellets were incubated with 1.5 mg/ml digitonin (Merck), spun, and washed with lysis buffer. The mitochondrial fraction was frozen in liquid nitrogen to grind with porcelain pestle and then in glass/glass homogenizer with a tight-fitting pestle in the lysis buffer. The lysates were spun (10,000*g* for 15 minutes), and the supernatant was used for the analysis of mitochondrial fraction.

The postmitochondrial and mitochondrial fractions were analyzed by SDS-PAGE electrophoresis and then transferred onto two nitrocellulose membranes (0.45 μm; Schleicher & Schuell, Dassel, Germany). The membrane was stained with Coomassie blue and washed with 5% acetic acid or blocked in 0.1 M sodium phosphate pH 7.5, 0.15 M NaCl, and 0.05% Twin-20 and then incubated with anti-TrpRS rabbit monospecific antibodies (overnight at room temperature). After washing, the membrane was incubated with goat antirabbit Fab fragments conjugated with horseradish peroxidase (Sigma) for 2 hours at room temperature and washed with buffer (50 mM Tris-HCl pH 7.5, 0.15 M NaCl). The reaction was developed with 0.05% 4-Cl-1-naphthol in 50 mM Tris-HCl, pH 7.5, and 0.05% hydrogen peroxide. Alternatively, after 12.5% SDS-PAGE of postmitochondrial extracts, the membrane was blocked by 5% bovine serum albumin (BSA; Sigma), 0.15 M NaCl, 10 mM Tris-HCl, pH 7.5, at 4°C overnight; incubated with anti-TrpRS IgG for 90 minutes, washed by 1% BSA, 0.15 M NaCl, 10 mM Tris-HCl pH 7.5, overnight at 4°C; and incubated with peroxidase-conjugated goat anti-rabbit Fab fragments for 1 hour. Peroxidase reaction was developed with 3,3′-diaminobenzidine (DAB).

Immunoprecipitation of TrpRS Labeled In Vivo *with [^{35}S]Methionine or [^{32}P]Orthophosphoric Acid*

Original MDBK and sublines treated with TrpRS inhibitors, tryptamine, or tryptophanol [20] were labeled *in vivo* with ^{35}S-methionine for 2.5 or 24 hours and tryptamine-resistant HeLa A cells [21] were labeled for 4.5 hours. Anti-TrpRS serum and nonimmune sera were used for immunoprecipitation of culture medium (HeLa A), monospecific polyclonal antibodies were used for immunoprecipitation of MDBK cell extracts insoluble in detergent (0.5% Triton X-100, 0.15 M NaCl, 50 mM Tris-HCl pH 7.5, 2 mM DFP at 0°C for 15 minutes), and detergent-soluble cells fractions were immunoprecipitated by anti-TrpRS IgG as described [20]. Detergent-insoluble fraction was washed three times with buffer for lysis, suspended in 5 mM Tris-HCl pH 7.5 and 2 mM DFP, and spun. Supernatants used for immunoprecipitation. Labeling with [^{32}P]orthophosphoric acid was conducted as described [20,21]. Detergent-soluble (2.5 or 48 hours of labeling) or postmitochondrial (5 hours of labeling) extracts of MDBK and tryptamine-treated sublines were immunoprecipitated with rabbit polyclonal antiserum or IgG or monospecific antibodies to TrpRS.

TrpRS Enzymatic Activity in MDBK Cells and Human Tissues

Human tissue extracts and cell extracts were assayed in tryptophan-dependent [^{32}P]PP_i-ATP exchange in buffer containing varied tryptophan concentrations (0-25 μM), 50 mM Tris-HCl pH 7.5, 10 mM $MgCl_2$, 0.2% dialyzed gelatin, 10 mM ATP, 3 mM PP_i, and [^{32}P]PP_i (6.9 mCi/mmol; Amersham, Buckinghamshire, United Kingdom). Postmitochondrial human extracts (400 μl each) were dialyzed before the assay against 50 mM Tris-HCl pH 7.5, 2 mM 2-ME, and 2.5 mM DFP (1 L) overnight and then against the buffer change (1 L for 3 hours at 4°C). The dialyzed tissue extracts (100 μg) were incubated in buffer for [^{32}P]PP_i-ATP exchange (200 μl for 12 minutes at 37°C) and then filtered and counted as described [20]. The count of control probes incubated without tryptophan for each extract was deducted.

Phospho–Amino Acid Analysis

After *in vitro* phosphorylation with [γ^{32}P]ATP, TrpRS was analyzed by PAGE. After autoradiography, the ^{32}P-TrpRS ~60-kDa bands were excised from the gel, boiled in 1% SDS (1 ml for 15 minutes), and spun, and supernatants were precipitated by acetone (5 ml). The dried pellets were hydrolyzed in 6 M HCl (1 ml for 90 minutes at 110°C). The hydrolysates were lyophilized and separated in two dimensions on thin-layer cellulose plates (Kodak, Rochester, NY) using electrophoresis in acetic acid/pyridine/water (87:2:911) at 1000 V in the first dimension and chromatography in *n*-butanol/formic acid/isopropanol/water (4:1:1:1) in the second dimension. The hydrolysates were also separated on thin-layer cellulose plates using electrophoresis in two dimensions as described [12,33]. Mobility of phospho–amino acid standards (Sigma) was visualized with ninhydrin.

Results and Discussion

Cancer Sera–Inducible Phosphorylation of TrpRS and Its Proteolytic Fragments

The cohort of cancer patients with solid malignant tumors of different types, metastatic disease and leukemia (Tables W1 and W2) and TBR revealed serum-inducible TrpRS phosphorylation (Figure 1). Blood sera of 11 of 15 healthy volunteers showed no stimulation of TrpRS phosphorylation (Figure 1). The serum of patient recovered after acute meningitis was abolished by endogenous TrpRS phosphorylation. The serum-inducible TrpRS phosphorylation was demonstrated in three healthy donors who have been later diagnosed with CRC, PC, or leukemia and in one healthy donor with papillomatosis (Table W3). Thus, serum-inducible TrpRS phosphorylation can be revealed years before clinical diagnosis of cancer.

Anti-TrpRS Sera as Chaperon-like Molecules to Restore Phosphorylation of Full-length TrpRS

To control the specificity of TrpRS phosphorylation, the polyclonal anti-TrpRS rabbit serum was examined, and it was found that it stimulated (10-fold) the phosphorylation of exogenous TrpRS in the presence of 2-ME (Figures 2*A* and W1). 2-ME was used to reduce disulfide bonds. 2-ME inhibits TrpRS phosphorylation, whereas anti-TrpRS serum-inducible phosphorylation is unaffected by 2-ME (Figure 2*B*). Consequently, anti–serum-inducible phosphorylation of full-length TrpRS was prevented in the absence of 2-ME (Figure 2*B*). In earlier studies, 2-ME inhibited phosphorylation of the microsomal polypeptides *in vitro* (>90% inhibition at 40 mM 2-ME) [34]. Both bTrpRS and hTrpRS contain six cysteine residues involved in the formation of disulfide bonds between two subunits. Cys62 is suggested to play a role in TrpRS angiogenic activity [35]. There are 24 serine-containing sites predicted for phosphorylation [36] in the hTrpRS sequence (GenBank accession no. EAW81703.1). In hTrpRS, Ser272 is close to Cys274 (Ser276 and Cys278 in bTrpRS). Some proteins can be denatured by 2-ME through its ability to cleave disulfide bonds. Therefore, the 2-ME–induced reduction of disulfide bonds in TrpRS inhibits its phosphorylation, whereas anti-TrpRS serum plays a role of chaperon refolding TrpRS and reactivating its phosphorylation. Note that the use of buffer containing 2-ME may lead to erroneous results if not freshly prepared. Specifically, the repeated freeze-thaw cycles of 2-ME containing PK buffer diminish the anti-TrpRS serum-inducible effect.

Effect of Anti-TrpRS Serum on Phosphorylation of TrpRS Forms

Stimulation of phosphorylation of 30- and 14-kDa TrpRS proteolytic fragments by antisera specific to TrpRS is 2-ME independent. After dialysis of TrpRS (48 hours), phosphorylation of the 30- and 14- to 17-kDa peptides is stimulated effectively by anti-TrpRS rabbit antisera but not nonimmune rabbit sera (Figure 3, *B* and *C*). Anti-TrpRS serum–stimulated phosphorylation of these fragments has been achieved in the minimal buffer containing Mn^{2+} and protease inhibitors (Figure 3*C*). Phosphorylation of 60- and 40-kDa TrpRS was not stimulated by anti-TrpRS or nonimmune rabbit sera in the absence of 2-ME. Anti-AFP and anti-TF polyclonal rabbit sera exerted no effect on TrpRS phosphorylation with or without 2-ME (Figure 3*B*). The ~100-kDa rabbit serum proteins were phosphorylated in the presence of TrpRS in anti-AFP, anti-TF, and nonimmune rabbit sera, whereas anti-TrpRS and TBR sera revealed no phosphorylation of 100-kDa serum proteins (Figure 3*D*).

Phosphorylation of 20-kDa TrpRS Proteolytic Polypeptide Is Stimulated by Anti-TrpRS IgG and Cancer Sera

Anti-TrpRS IgG abolished phosphorylation of 60-kDa TrpRS (Figure 1*A*) but stimulated phosphorylation of the ~20-kDa fragment in the presence of 2-ME (50 mM; Figure 4*A*). This fragment is not produced by IgG-associated hydrolysis as evident from Coomassie staining

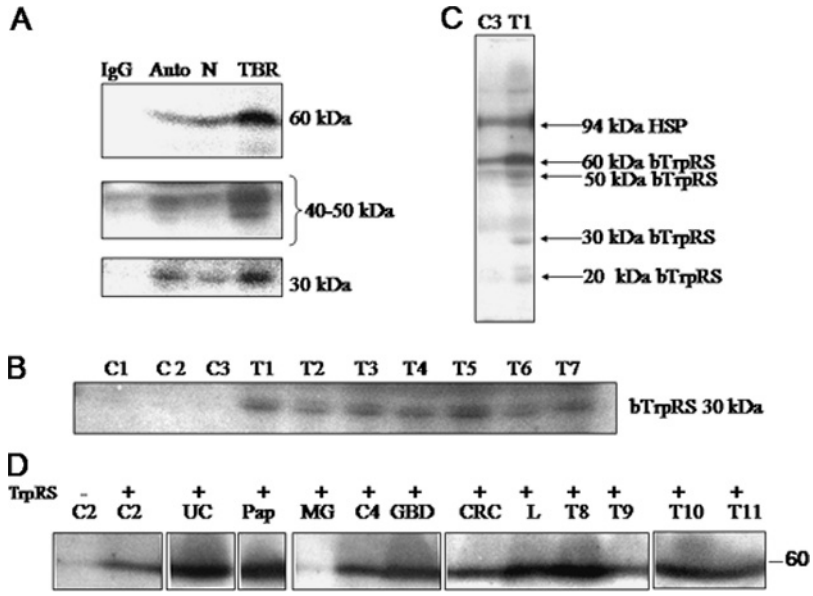

Figure 1. Serum-inducible phosphorylation of purified bTrpRS (selected human and rabbit sera). (A) TrpRS endogenous phosphorylation (auto) is stimulated by TBR serum but not serum of normal rabbit (N) in the presence of Mg^{2+}, Mn^{2+}, and 2-ME. Anti-TrpRS IgG totally abrogated (60 and 30 kDa) or decreased (50 kDa) phosphorylation of TrpRS and its proteolytic polypeptides. (B-D) Serum-inducible TrpRS phosphorylation. (B) Phosphorylation of 30-kDa TrpRS polypeptide in the presence of blood sera from healthy donors (C) (donor 1 [C1], F; donor 2 [C2], M; donor 3, M [C3]) and cancer patients (T) (stomach cancer, multiple metastases in liver, bladder, ascites, F [T1]; chondroma, rib no. 4 right side, fast-growing, M [T2]; testicular seminoma, left side, stage 3, M [T3]; lung cancer, upper lobe of left lung, stage 3, M [T4]; cancer colli uteri [CC], stage 3, F [T5]; bladder cancer, stage 3, M [T6]; lung cancer, right lung stage 4, metastasis in spinal cord, M [T7]). (C) Comparison of representative phosphorylation profiles of TrpRS in the presence of sera from donor 3, M (C3) and patient with stomach cancer, multiple metastases in liver, bladder, ascites, F (T1). (D) TrpRS phosphorylation after addition of selected human sera. Healthy donor, M (C2); uterine cancer, underwent radical surgery, radiation therapy 8 years before testing, no cancer at the time of testing, F, RBP (UC); healthy donor (papilloma removed), F (Pap); healthy donor, acute meningitis, 1.5 years before the testing, M (MG); healthy donor, M, FPT (C4); gallbladder disease at the time of testing, F, YSM (GBD); colorectal cancer, after surgery, F, LPM (CRC); leukemia (L); squamous cell lung cancer, central location of right lung, stage 4, moderately differentiated, M (T8); urinary bladder cancer, recurrent, stage 3, F (T9); stomach cancer, F (T10); stomach cancer, 4 stage, M (T11). Then, 12.5% SDS-PAGE followed by autoradiography. F indicates female; M, male.

(Figure 4*A*). Phosphorylation of this fragment is stimulated also by TBR serum and sera from six of seven cancer patients but not by sera from healthy donors (Figure 4*B*). PK assay is conducted in the presence of protease inhibitor. No accumulation of the 20-kDa fragment was detected by Coomassie staining after incubation with cancer sera (Figure 4*B*). In previous studies, the bTrpRS fragments were produced by limited proteolysis with trypsin by the following scheme: 2 × 60 kDa → 2 × 40 kDa → 2 × 24 kDa → 2 × 14 kDa. The carboxy-terminal 40-kDa fragment and amino-terminal 20-kDa fragments produced were also due to endogenous proteolysis [37]. The activity of full-length bTrpRS in aminoacylation is inhibited by anti-TrpRS polyclonal antibodies. However, bTrpRS activity in aminoacylation was unaffected by binding of antibodies to N-terminal 20-kDa TrpRS fragment. In our earlier study, some sera of cancer patients contained anti-TrpRS IgG [38]. Thus, anti-TrpRS IgG can affect phosphorylation of TrpRS *in vivo* in human. Serum-stimulated phosphorylation sites were revealed also in another translational protein—eukaryotic translation initiation factor 4GI [39]. Thus, anti-TrpRS IgG is suggested to be a factor or cofactor in the stimulation of TrpRS phosphorylation by cancer sera. All molecular chaperones known to date are protein molecules whose three-dimensional structures are believed to play a key role in the mechanism of substrate recognition and subsequent assistance to folding. A previous study demonstrated that the monoclonal antibody to bTrpRS is able to disaggregate helical fibrils self-assembled by TrpRS N-terminal peptide [23]. In the stimulation of TrpRS phosphorylation, human cancer sera, TBR serum, as well as anti-TrpRS antisera and IgG may work as chaperone-like molecules to play a role in the molecular recognition of TrpRS and subsequent assistance in refolding.

Casein Works as Chaperons for TrpRS in the Presence of 2-ME

Casein is examined here as a possible substrate for TrpRS-associated PK. Surprisingly, the chaperone-like activity in refolding of TrpRS by casein is demonstrated in the presence of 50 mM 2-ME, which promotes the dissociation of TrpRS subunits (Figure W2*A*). Such activity was not detected in BSA, protein A, and histones (Figure W2, *A* and *B*). A cyclic AMP (cAMP)-independent weak phosphorylation of casein is catalyzed by TrpRS–PK (Figure W3). Most, but not all, of the casein proteins exist in a colloidal particle known as the casein micelle. αs-Casein not only prevents the formation of huge insoluble aggregates but also inhibits accumulation of soluble aggregates of appreciable size. Unlike other molecular chaperones, this protein solubilizes hydrophobically aggregated proteins. This protein seems to have some characteristics of cold shock protein, and its chaperone-like activity increases with a decrease in temperature [40]. α-Casein micelles show not only molecular chaperone-like aggregation inhibition properties but also protein refolding activity from the denatured state [41]. TrpRS is susceptible to aggregation *in vitro* and in the human brain [23].

Synergistic Effects of cAMP and 2-ME on TrpRS Phosphorylation

A possible cAMP dependence of TrpRS is further examined in the phosphorylation assay. cAMP (100 μM) in combination with 2-ME (50 mM) abolishes endogenous TrpRS phosphorylation (Figure 2*A*), whereas cAMP alone has no such effect (Figure W3). 2-ME alone inhibits TrpRS phosphorylation but to a lesser extent than in combination with cAMP (Figure 2, *A* and *B*). Apparently, cAMP enhances the effect of 2-ME. 2-ME stimulates oxidative dissociation of TrpRS subunits with concomitant impairment of TrpRS phosphorylation. cAMP enhances 2-ME–induced inhibition of TrpRS phosphorylation that was partially restored by chaperon-like effects of anti-TrpRS serum and casein (Figures 2, *A* and *B*, and W2). The synergistic effect of cAMP and 2-ME can be explained by cAMP-mediated intersubunit disulfide cross-linking that was earlier proposed for *Escherichia coli* protein [42]. Incorrect disulfide TrpRS intersubunit cross-linking may lead

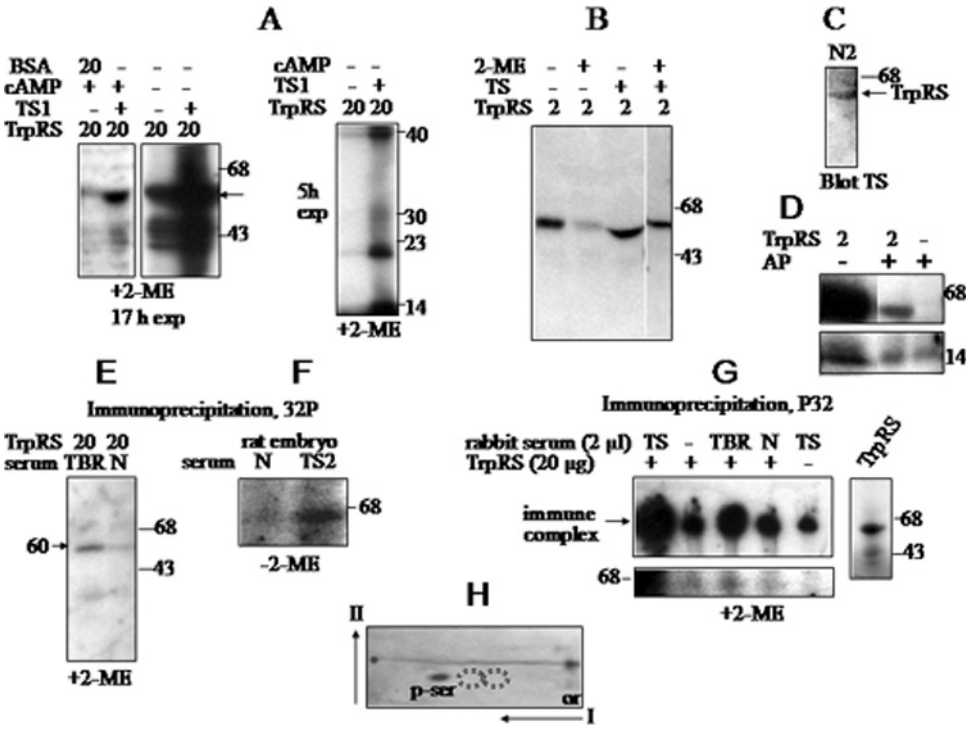

Figure 2. Serum-inducible TrpRS phosphorylation (rabbit sera). (A) Anti-TrpRS rabbit serum (TS) stimulates bTrpRS phosphorylation in the presence of 50 mM 2-ME. cAMP (100 μM) repressed TrpRS-PK and anti-TrpRS serum-inducible TrpRS phosphorylation. Left and right panels show 17 and 5 hours of exposure of x-ray films, respectively. (B) Phosphorylation of purified full-length bTrpRS inhibited by 2-ME (50 mM) and stimulated by anti-TrpRS serum (TS) in the presence of 2-ME (50 mM), 30 minutes of x-ray film exposure. (C) TrpRS secretion into rabbit sera. Anti-TrpRS (TS1 and TS2) and nonimmune (N1, N2) rabbit sera (10 μl each) analyzed by 12.5% SDS-PAGE followed by immunoblot with TS antiserum (1:100). Immunoperoxidase reaction developed with DAB. All four sera contained TrpRS (N2 > N1 > TS1 = TS2). (D) Alkaline phosphatase from *E. coli* (AP) inhibits phosphorylation of TrpRS and its 14-kDa peptide. TrpRS (2 μg) incubated with 2.5 μl of AP (72 U/mg, 215 U/ml, 40 minutes at 25°C) and then phosphorylated in PK buffer (20 μl, 20 mM Tris-HCl pH 7.2, 2 mM $MnCl_2$, 5 mM $MgCl_2$, 1 mM 5′AMP, 3 mM DFP, 3 μl of [γ-^{32}P]-ATP [2-3000 Ci/mmol, 1 mCi/0.2 ml]). (E) TrpRS immunoprecipitation with TBR serum followed by phosphorylation with [γ-^{32}P]ATP (see Materials and Methods section). (F) Rat embryo washed in Hank's buffered solution, cut with scissors in the same buffer, washed, homogenized in glass/glass homogenizer in 5 ml of lysis buffer (0.5% Triton X-100, 0.14 M NaCl, 50 mM Tris-HCl pH 7.2, 3 mM DFP, 3 mM PMSF, 0.5% aprotinin) with DFP (2 μl), and spun. The supernatant (600 μl) was preincubated with cocktail of nonimmune sera N1 and N2 (6 μl of each serum), overnight at 4°C, and 10% protein A *S. aureus* (50 μl) was added in RIPA buffer for 30 minutes at 37°C, spun, and washed in the same buffer. The supernatants (100 μl/probe) were incubated with TS2 or N rabbit sera (3 μl) overnight; 10% protein A *S. aureus* (20 μl) was added to each probe for 40 minutes at 37°C. (G) Purified bTrpRS immunoprecipitated by rabbit polyclonal anti-TrpRS serum (TS) or TBR serum. Immunoprecipitation with nonimmune rabbit serum (N) was undetectable. After the reaction (100 μl of PBS for 50 minutes at 37°C), immunoprecipitates were incubated with 20 μl of 10% protein A *S. aureus* (immunoprecipitation) suspended in lysis buffer (0.5% Triton X-100, 0.14 M NaCl, 50 mM Tris-HCl pH 7.2, 3 mM DFP, 3 mM PMSF, 0.5% aprotinin) for 30 minutes at 37°C. Immunoprecipitates (pellets) were washed three times with 1 ml of ice-cold RIPA buffer (0.15 M NaCl, 0.01 M sodium phosphate, pH 7.2, 1% NP-40 [Sigma], 1% sodium deoxycholate [Sigma], 0.1% SDS, and 3 mM PMSF). Pellets were suspended in 1 ml of PK buffer (20 mM Tris-HCl [Calbiochem], pH 7.2, 2 mM $MnCl_2$ [Fluka], 1 mM 5′AMP, 50 mM 2-ME, and 50 μM EDTA) and spun, and each pellet was suspended in PK buffer (20 μl) with 10 μCi of [γ-^{32}P]-ATP (2-3000 Ci/mmol, 400 μCi/0.1 ml of water) for 10 minutes at 37°C. Laemmli sample buffer (boiling for 5 minutes) was analyzed on 4% SDS-PAGE (immune complex) or 10% SDS-PAGE. TrpRS was phosphorylated without previous immunoprecipitation (10% SDS-PAGE; right). X-ray exposure for 21 hours (immunoprecipitation) and 2 hours (TrpRS). (H) Two-dimensional phospho–amino acid analysis. ^{32}P-TrpRS was excised from gel (10% SDS-PAGE) and analyzed using electrophoresis (9 cm from start (or)) in the first dimension (I) and chromatography in the second dimension (II). Phosphoserine (p-ser) is detected in ^{32}P-TrpRS and serum-inducible ^{32}P-TrpRS. Ninhydrin-stained phosphothreonine and phosphotyrosine are encircled.

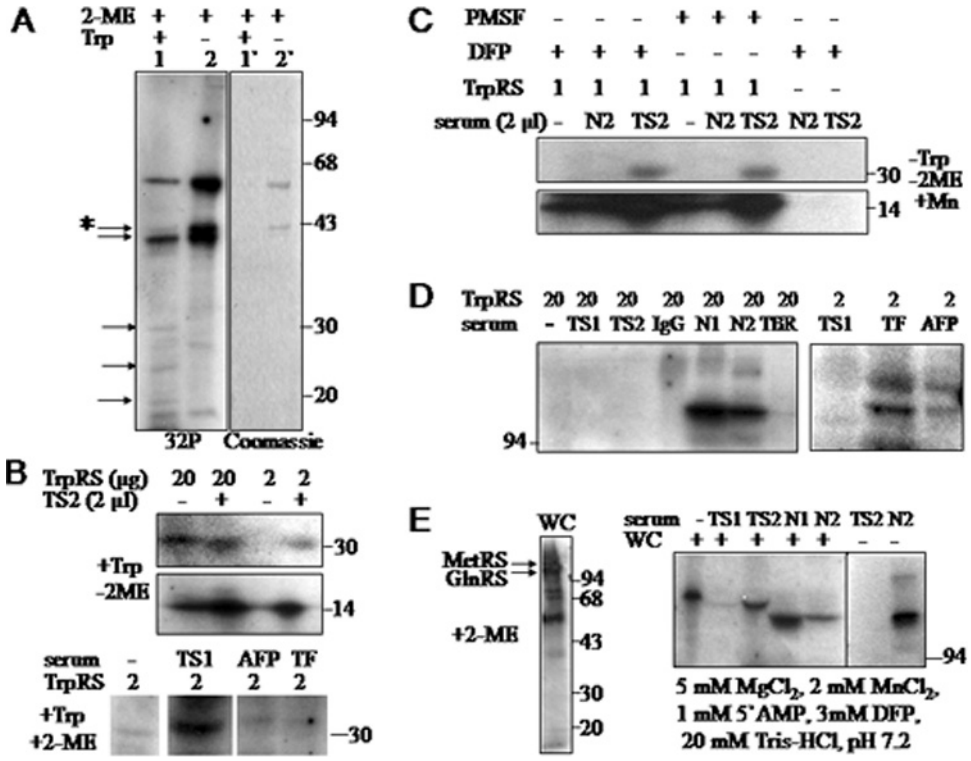

Figure 3. Anti-TrpRS serum stimulates phosphorylation of TrpRS proteolytic fragments but not components of ARS complex. (A) Phosphorylation of TrpRS polypeptides stimulated (arrows) or inhibited (arrow with asterisk) by 10 μM tryptophan: autoradiography (1, 2) and Coomassie staining (1′, 2′). (B) Effect of rabbit antisera to bTrpRS (TS), AFP, and Thomsen-Friedenreich antigen (TF) on phosphorylation of the 30- and 14-kDa polypeptide. (C) Serum-inducible phosphorylation of 30- and 14-kDa polypeptides with anti-TrpRS rabbit serum (TS2) but not with nonimmune rabbit serum (N) in the presence of protease inhibitors, 3 mM DFP or 3 mM PMSF, 2 mM $MnCl_2$, and 20 mM Tris-HCl, pH 7.2. (D) Phosphorylation of 100-kDa endogenous rabbit serum polypeptides in the presence of TrpRS. Rabbit sera used were as follows: RSV-induced tumor (TBR), anti-TrpRS (TS1, TS2), anti-TrpRS IgG, nonimmune (N1, N2), anti-AFP, and anti-TF. (E) Decreased phosphorylation of the components of multienzyme ARS complex (WC; 20 μg/sample) in the presence of anti-TrpRS (TS1, TS2) or nonimmune rabbit (N1, N2) sera (2 μl/sample). Phosphorylated GlnRS and MetRS (~105 kDa) assigned as described [47]. A (left) and B to E show autoradiographs. TrpRS (1, 2, or 20 μg) and rabbit sera (2 μl) are included in samples (indicated).

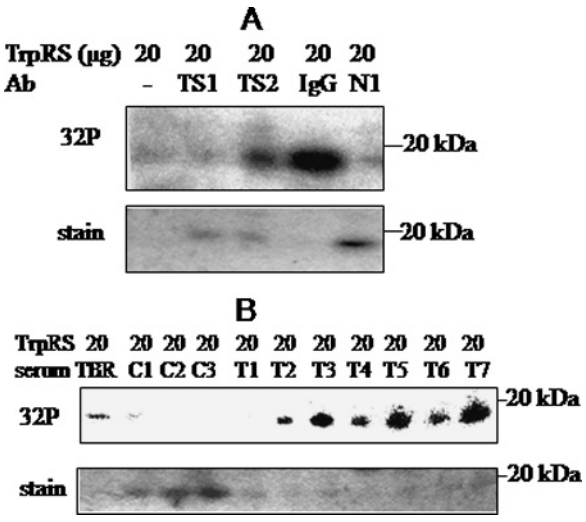

Figure 4. Phosphorylation of 20-kDa TrpRS proteolytic polypeptide is stimulated by anti-TrpRS IgG (A) and cancer sera (B). Sera obtained from the human cohort (B) described in the legend to Figure 1*B*: autoradiography (^{32}P) and Coomassie staining (stain). Rabbit samples are shown in A and B (TBR); human samples are shown in B (C1 to T7).

in aggregation, which impairs TrpRS phosphorylation. Cerebrospinal fluid cAMP levels are increased in AD [43]. TrpRS aggregates were detected in the brain of patients with AD [23].

Effect of Tryptophan on Phosphorylation of TrpRS Fragments

The TrpRS substrate, tryptophan, protects TrpRS from dissociation and inactivation [44], whereas tryptophan analogs and competitive TrpRS inhibitors, tryptamine and tryptophanol, induce TrpRS aggregation *in vivo* [20]. Therefore, a possible effect of tryptophan on TrpRS phosphorylation was examined in the presence of 2-ME. Phosphorylation of 20-, 25-, 30-, and 40-kDa TrpRS fragments seems to be stimulated by tryptophan (Figure 3*A*). In a previous study, the polypeptides with molecular masses of approximately 40 and 30 kDa were revealed in elastase and CNBr-generated bTrpRS fragments, respectively [45]. A common increase of free plasma tryptophan in human cancer may be implicated as cofactor in serum-inducible TrpRS phosphorylation.

Secreted TrpRS in Rabbit Sera

TrpRS was secreted [24]. To explore the possibility that TrpRS-PK is involved in serum-inducible phosphorylation, immunoblot analysis of TrpRS was conducted. The ~58-kDa TrpRS is detected in two

nonimmune and two anti-TrpRS rabbit sera by anti-TrpRS polyclonal antibodies. The TrpRS level is lower in anti-TrpRS sera than in nonimmune rabbit sera (Figure 2*C*).

Immunoprecipitation of TrpRS by TBR

TBR serum stimulates TrpRS phosphorylation (Figure 1*A*). Moreover, TBR serum immunoprecipitates PK associated with TrpRS (Figure 2, *E* and *G*). TrpRS-PK is immunoprecipitated also from rat embryo by anti-TrpRS serum but not by nonimmune rabbit serum (Figure 2*F*). Because TBR serum contains antibodies against RSV virion structural proteins, it may contain antibodies to TrpRS that packed in RSV virion with its cognate $tRNA^{trp}$ [9]. Endogenously phosphorylated TrpRS and TrpRS immunoprecipitated by TBR serum or anti-TrpRS serum contain phosphoserine (Figure 2*H*). A cross-immunoreactivity between TrpRS and src could also cause immunoprecipitation of TrpRS by TBR serum. To examine this possibility, the TrpRS and src protein sequences have been compared. Although no significant similarity between hTrpRS (GenBank accession no. EAW81703.1) and human c-src protein (GenBank accession no. AAH11566.1) was detected, the 11-amino acid (aa) peptides near the carboxyl termini of hTrpRS 399/SFMYLTFFLED/409 and human c-src 511/TFEYLQAFLED/521 show 64% identity (7/11 aa). This homologic peptide is adjusted and partially overlapped with conformation-dependent TrpRS antigenic epitope that we previously mapped at Asp409-Met425 [23]. The peptide lies 5 aa upstream of the c-src major phosphorylation site Tyr527. This sequence is not present in pp60 v-src (Swiss-Prot no. P00524.5) but is present in bTrpRS (National Center for Biotechnology Information no. NP_776643.1). Phosphorylation of pp60 c-src at Tyr527 suppresses its tyrosine kinase activity and transforming potential [46]. Mapping of TrpRS epitope in the region, which is similar to c-src sequence, suggests that anti-TrpRS conformation-dependent antibody may bind c-src and modulate kinase activity specific to c-src major site Tyr527 responsible for transformation.

Phosphorylation of Multienzyme Complex of ARS

Other ARS are also phosphoproteins. Therefore, it is of interest to examine whether phosphorylation of synthetases of the ARS complex was affected by serum. The multisynthetase core complex comprising seven ARS underwent self-phosphorylation. The ARS complex from rabbit liver possesses an endogenous PK activity (Figure 3*E*). Phosphorylation of the ~100-kDa doublet is detected in the complex in agreement with a previous study [47]. These proteins are attributed as glutaminyl-tRNA synthetase (GlnRS) and methionyl-tRNA synthetase (MetRS). The phosphorylation of GlnRS and MetRS was suppressed by anti-TrpRS rabbit sera and abolished by nonimmune rabbit sera. Phosphorylation of other components of the multienzyme complex was unaffected by the rabbit sera. In an earlier study, PKC phosphorylated glutamyl-tRNA synthetase but not MetRS and GlnRS [29]. Phosphorylation *in vivo* is accompanied by a 38% ± 10% reduction in aminoacylation activity of partially purified glutamyl-tRNA synthetase assayed *in vitro*. Serine phosphorylation of a multisynthetase complex component, glutamyl-prolyl tRNA synthetase, by cyclin-dependent kinase 5 regulates translational control [48].

Histone-Specific PK in Human Sera

In a previous study, TrpRS-specific PK phosphorylates histones [12]. Therefore, it is of interest to examine phosphorylation of histones in the presence of human sera affecting TrpRS phosphorylation (Tables W4–W6). Histones underwent phosphorylation in the presence of earlier tested (Figure 1) and yet untested human sera. Donor sera, which do not affect TrpRS phosphorylation, phosphorylate strongly histones, mainly histone H2B (Figure 5, *A-C*). Earlier tested sera of donors with gallbladder disease (GBD) and papilloma (Pap) and TrpRS-untested sera of patients with psoriasis (Psr) phosphorylate also histone H4. Endogenous phosphorylation of histones was undetectable (Figure 5*E*). Endogenous phosphorylation of serum polypeptides of low molecular mass overlapping with the molecular mass of histones H2A, H2B, H3, and H4 is commonly undetectable (Figure 5*D*) unless serum proteins are heavily proteolyzed on repeated freeze-thaw cycles. Normal human serum partially loses histone-specific PK activity on repeated freeze-thaw cycles (second to third cycles). Phosphorylation of histones by cancer sera and serum of healthy donor diagnosed later with CRC (C4) is low or undetectable (Figure 5, *A-C*). The histone-specific PK serum activity is low in 8 but normal in 2 of 10 hospitalized patients with pneumonia (Figure 5, *C* and *E*). Sera of patients with acute myocardial infarction (3/3 patients) and stomach ulcer (1 patient) had undetectable histone-specific PK activity.

Histone-Specific PK in Rabbit Sera

Phosphorylation of histones was examined also in the presence of nonimmune rabbit sera, anti-TrpRS polyclonal rabbit sera, anti-TrpRS IgG, anti-AFP polyclonal rabbit antiserum, and anti-TF antigen polyclonal rabbit serum (Figures 6 and W3). Nonimmune sera, anti-AFP, and anti-TF sera strongly phosphorylated histones in the presence of Mg^{2+} and Mn^{2+}. Phosphorylation of histone H2B in the presence of Mg^{2+} alone was lower than in the presence of Mn^{2+} alone and was highest in the presence of both Mg^{2+} and Mn^{2+} (Figure 6*D*). Phosphorylation of histone H2B with anti-TrpRS rabbits was low or undetectable (Figure 6*D*). Anti-TrpRS IgG showed no histone-specific PK activity in the presence of Mg^{2+} and Mn^{2+} (Figures 6*E* and W3). Thus, in contrast to TrpRS serum-inducible phosphorylation, histone phosphorylation has not been induced by anti-TrpRS sera but was stimulated by other rabbit sera, which do not visibly affect TrpRS phosphorylation. These data indicate that a link exists between TrpRS and histones in serum-inducible phosphorylation.

Endogenous Human Serum Phosphorylation

To control the "background" signal in human serum phosphorylation, endogenous phosphorylated proteins were examined in the presence of Mg^{2+} and Mn^{2+} and in the absence of exogenous substrates. The ~100-kDa phosphopolypeptide/s was found to be present in sera of healthy individuals and absent in most cancer patients (Figure 5*E*, *arrows*).

Immunoprecipitation of ^{35}S In Vivo*–Labeled TrpRS from Culture Medium*

To examine if TrpRS is secreted by cancer cells, the culture medium of ^{35}S-labeled tryptamine-treated subline HeLa-A expressing TrpRS with a longer half-life (>5 hours) than original HeLa (<2 hours) [21] was immunoprecipitated. Several labeled fragments were immunoprecipitated by anti-TrpRS antiserum from HeLa-A cell culture medium after *in vivo* metabolic labeling (4.5 hours) with [^{35}S]methionine (Figure W4*A*). These data confirm that TrpRS is secreted by human cancer cells.

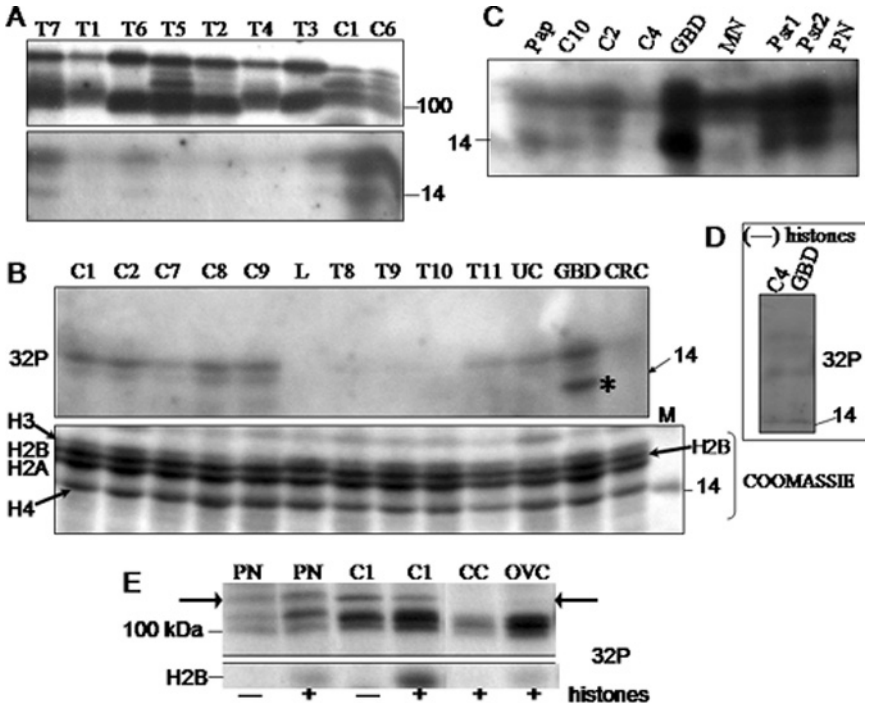

Figure 5. Serum-inducible phosphorylation of histones and endogenous phosphorylation of p100 in selected human samples. (A) Samples of healthy women (C1 and C6); cancer serum samples (T1-T7) of females (F) and males (M) correspond to numbers as in Figure 1*C*: stomach cancer (T1), multiple metastases in liver, bladder, ascites, F; chondroma, rib no. 4, right side, fast-growing, M (T2); testicular seminoma, left, stage 3, M (T3); lung cancer, upper lobe of left lung, stage 3, M (T4); CC (cancer colli uteri) stage 3, F (T5); bladder cancer, stage 3, M (T6); lung cancer, right lung stage 4, metastasis in spinal cord, M (T7). Upper panel, ^{32}P autoradiography of 100-kDa phosphopolypeptides; lower panel, histone phosphorylation. (B) Histone phosphorylation by selected human sera revealed by ^{32}P autoradiography (upper panel) and Coomassie staining (lower panel) of the same SDS-PAGE. The positions of histones H2A, H2B, H3, and H4 are indicated at the side. Serum samples of healthy individuals: C1 (F); C2 (M); C7 (M); C8 (F); C9 (M); leukemia (L); squamous cell lung cancer, central location of right lung, stage 4, moderately differentiated, M (T8); urinary bladder cancer, recurrent, stage 3, F (T9); stomach cancer, F (T10); stomach cancer, 4 stage, M (T11); uterine cancer, 8 years before the testing, after surgery, after radiation therapy, no cancer, F (UC); gallbladder disease, F (GBD). Histone H4 phosphorylation (asterisk); colorectal cancer, after surgery, F (CRC). Probe included 20 μg of histones (10 mg/ml, H_2SO_4 extraction), serum (2 μl/sample), 18 μl of PK buffer (2-ME, Mn^{2+}, 5′AMP), [γ-^{32}P]ATP (5 μCi/sample for 15 minutes at 37°C). (C) ^{32}P autoradiography of histone phosphorylation by selected sera of noncancer individuals. Noncancer individual, papilloma removal, papillomatosis in family (mother, sister), F (Pap); noncancer individual, cervical erosion 8 to 9 years before testing, papillomas, papillomatosis in family, F (C10); healthy individual, M (C2); healthy individual, M (C4); gallbladder disease, F (GBD), GBD in family (mother); healthy individual, acute meningitis 1.5 years before the testing, M (MG); psoriasis case 1 (Psr1), psoriasis case 2 (Psr2); pneumonia, M (PN). (D) ^{32}P autoradiography of serum phosphorylation without exogenous histones. Note that none or only marginal phosphorylation of low–molecular weight peptides of 14 to 18 kDa was detected. Healthy individual, M (C4); individual with gallbladder disease, F (GBD). (E) Comparison of serum-inducible phosphorylation of endogenous p100 and exogenous histone H2B by selected representative samples from a healthy individual (C1), a pneumonia case (PN), and individuals with OVC and CC. ^{32}P autoradiography of phosphorylation with (+) or without (−) histones.

Refolding of TrpRS Aggregated and Labeled In Vivo

Refolding and stability of TrpRS from detergent-insoluble fraction. Here, *in vitro* refolding of TrpRS-labeled *in vivo* was studied in the original MDBK cell and sublines treated with tryptophan analogs [20]. After *in vivo* labeling of MDBK cells with [^{35}S]methionine (24 hours), detergent-insoluble extracts were incubated with anti-TrpRS monospecific antibodies or with the immune complex of purified unlabeled bTrpRS with anti-TrpRS monospecific antibodies (TrpRS–anti-TrpRS). The level of ^{35}S-TrpRS immunoprecipitated with TrpRS–anti-TrpRS immune complex exceeds significantly the level of immunoprecipitation with antibodies alone. Apparently, renaturation of aggregated TrpRS is stimulated by chaperone-like or cochaperone activity of TrpRS–anti-TrpRS immune complex in detergent-insoluble fraction, which contains aggregated proteins (Figure W4*B*). It seems that the level of TrpRS aggregation is underestimated in conventional immunoprecipitation that uses antibodies that are not pretreated with antigen. After 24 hours of labeling (detergent-insoluble fraction), TrpRS was undetectable or was decreased in the treated cells, whereas TrpRS level was unchanged in control MDBK in comparison with the level detected after 2.5 hours of labeling (Figure W4*B*). These data indicate that TrpRS turnover increased, whereas its half-life decreased after prolonged tryptamine or tryptophanol treatment of MDBK. Both tryptamine and tryptophanol are carboxyl analogs of tryptophan and TrpRS inhibitors. The bTrpRS dissociation constants, K_s calculated from the Scatchard plots are 0.95 μM for tryptophan and 1.8 μM for tryptamine [44].

TrpRS catalyzed tryptophan-dependent ATP-[^{32}P]PP$_i$ exchange. To correlate TrpRS enzymatic activity with TrpRS aggregation and phosphorylation, the ATP-PP$_i$ exchange was examined in detergent-soluble cell extracts of untreated MDBK and tryptamine-treated MDBK

subline. The enzymatic activity is ~2.5-fold higher in tryptamine-treated cells compared with control cells (Figure W5).

TrpRS refolding in detergent-soluble fraction of cells treated with TrpRS inhibitors. In the same treated cells, the amount of immunoprecipitated ^{35}S-labeled TrpRS (50-kDa excised band) is ~10 times higher compared with control cells after 2.5 hours of labeling (Figure 4, T2 in panel *B* corresponds to TN3 in panel *C*, both indicated with asterisks). A dramatic difference in ^{35}S-TrpRS (2.5 hours of labeling) immunoprecipitated from detergent-soluble fractions is detected between cells treated with inhibitors and control cells when immune complex (anti-TrpRS IgG with purified unlabeled TrpRS) was used for immunoprecipitation (Figure W4*C*). When anti-TrpRS IgG was used alone for immunoprecipitation, the difference between control and treated was less dramatic in ^{35}S-TrpRS level because TrpRS–anti-TrpRS IgG enhances TrpRS immunoprecipitation in treated cells and decreases in control. These results suggest that treated cells contain a high amount of aggregated TrpRS, which were disaggregated by the TrpRS–anti-TrpRS IgG immune complex. The disaggregating ability of mAb to TrpRS was demonstrated in a previous study [23]. The level of TrpRS aggregation in cells treated with tryptamine or tryptophanol is underestimated by conventional immunoprecipitation. Thus, the proportion of enzymatically inactive TrpRS in tryptamine-treated cells may be higher than 75%, a percentage estimated using conventional immunoprecipitation with antibodies alone (Figure W4) and tryptophan-dependent ATP-PP$_i$ exchange (Figure W5).

Equilibrium of phosphorylated, enzymatically active, and ^{35}S-labeled TrpRS. Analysis of enzymatic activity (AT-PP$_i$ exchange), ^{35}S-labeled, and ^{32}P-labeled TrpRS in control MDBK and cells treated with TrpRS inhibitors reveals that a significant proportion of TrpRS (75%) is enzymatically inactive and, at the same time, nonphosphorylated in treated cells (Figure W5). The level of ^{32}P-TrpRS immunoprecipitated from the detergent-soluble fraction of control MDBK cells is reduced after incubation with TrpRS–anti-TrpRS, suggesting that control cells contain no aggregated phospho-TrpRS (Figure W5*A*). Phosphorylated TrpRS is detected at a higher level in the detergent-soluble fraction compared to postmitochondrial fraction (Figure W5*B*). ^{32}P TrpRS detected in the postmitochondrial fraction of treated cells but was undetectable in the control MDBK. Alkaline phosphatase abolished TrpRS *in vivo* phosphorylation (Figure W5*A*). It has become increasingly clear in recent years that amino acids can stimulate a signal transduction pathway resulting in the phosphorylation [49]. The present data show that amino acid analogs can effect phosphorylation in a tryptophan competitive manner. The effects of TrpRS analogs are physiology relevant because tryptamine presents in human blood and tissue [50,51]. The epidemiology data show that AD and cancer strike rarely the same person [52]. Taken together, the tryptamine-induced AD model of neurodegeneration [22,24] and present data (Figure W4) prompt the suggestion that the chaperone-like disaggregating activity of TrpRS–anti-TrpRS immune complex may prevent AD in cancer patients. Tryptamine and tryptophanol induce accumulation of aggregated, nonphosphorylated, and enzymatically inactive TrpRS in cells.

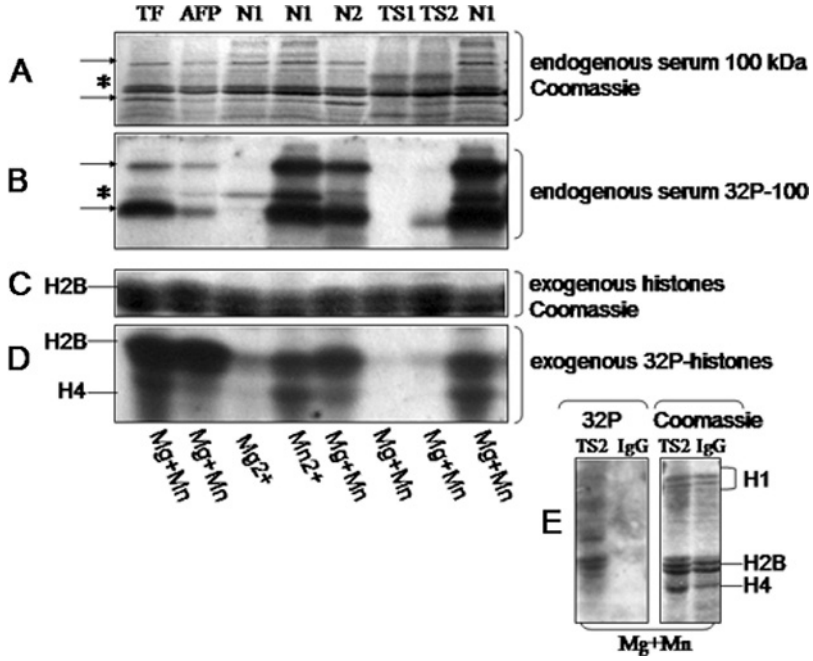

Figure 6. Effect of magnesium (Mg^{2+}) and manganese (Mn^{2+}) on histone phosphorylation by immune and nonimmune rabbit sera. Sera (2 μl) of rabbits immunized with TF antigen, AFP, bTrpRS (TS1 and TS2) and nonimmune rabbits (N1 and N2) used for *in vitro* phosphorylation of purified histones with [γ-^{32}P]ATP in the presence of Mg^{2+} or Mn^{2+} or both Mg^{2+} and Mn^{2+} (Mg + Mn): Coomassie staining (A, C) and ^{32}P labeling (B, D). A and B show high–molecular weight polypeptides (≥100 kDa), C and D show low–molecular weight polypeptides (14-18 kDa) at 15% SDS-PAGE. Arrows point at Mn^{2+}-dependent phosphorylation, and asterisks indicate Mg^{2+}-dependent phosphorylation of serum polypeptides (A, B). H2B and H4 are exogenous histones (C, D). (E) Low level of IgG-independent anti-TrpRS serum-inducible (TS2) histone phosphorylation (^{32}P). Positions of histones H1, H2B, and H4 are also indicated. Autophosphorylation of anti-TrpRS IgG, histones, and 14- to 18-kDa endogenous serum polypeptides is undetectable.

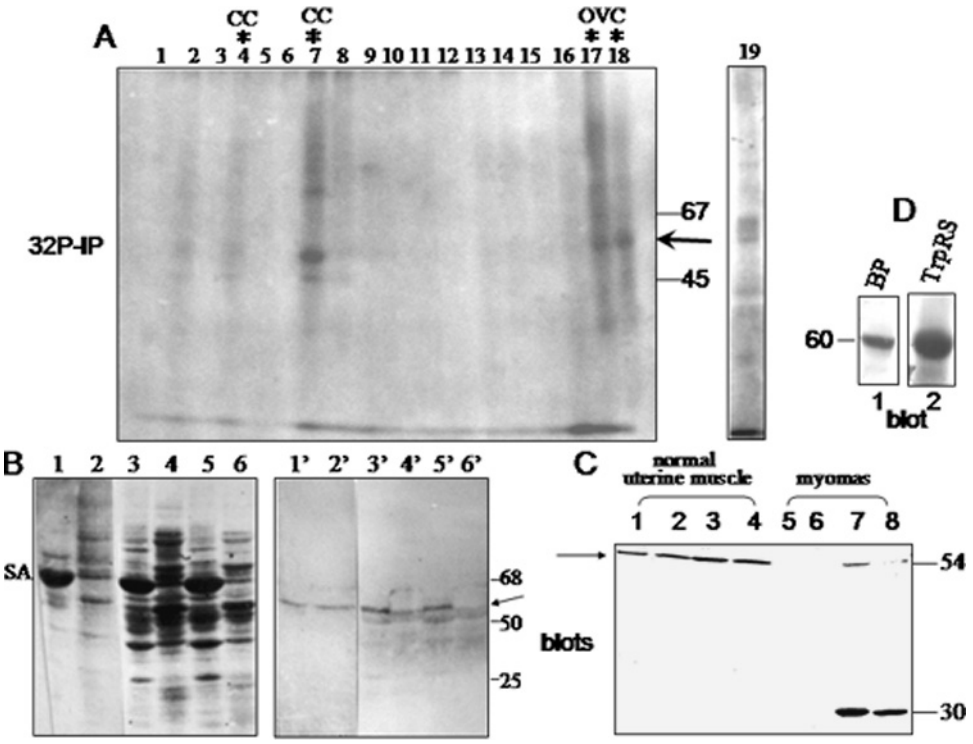

Figure 7. Phosphorylated TrpRS is immunoprecipitated from postsurgical human tissue samples. (A) Postmitochondrial extract (50 μg) phosphorylation (9 μCi of [γ-^{32}P] ATP/sample, 10 mM Mg^{2+} for 2 minutes at 37°C), termination (20 mM EDTA), and immunoprecipitation (IP) with rabbit monospecific polyclonal antibodies to bTrpRS (1 hour). Immunoprecipitates of normal muscle from individuals with uterine cancer stage 1 (1); normal uterine muscle (2); normal uterine muscle from individual with necrotic myoma (3); normal uterine muscle from individual with CC (4); normal epithelium of uterine (5); normal epithelium from individual with necrotic myoma (6); epithelium of individual with CC (7); normal placenta (8); liver from individual with hepatitis B/serum hepatitis (9); four cases of myomas (10-13) (myoma, 10; fibromyoma, 11; myoma of individual with endometrial cancer, 12; fibromyoma, 13); corpus uterine cancer, three cases (14-16); OVC, two cases (metastatic ovarian cancer 1, 17; ovarian cancer 2, 18); and normal bovine liver (19) separated (12.5% Laemmli SDS-PAGE for 12 hours). Different tissue samples were obtained from the same individual: 2 and 5, 3 and 6, and 4 and 7. (B) Immunoblot of postmitochondrial (1, 3, 5, 1′, 3′, 5′) and mitochondrial (2, 4, 6, 2′, 4′, 6′) extracts of OVC cases (3-6, 3′-6′) and normal placenta (1, 2, 1′, 2′) with anti-TrpRS antibodies. Nitrocellulose membrane was stained with Coomassie blue (1-6) or incubated with antibodies (1′-6′). (C) Immunoblot of postmitochondrial extracts (50 μg) from normal uterine muscle (4 cases) and myomas (4 cases) with anti-TrpRS antibodies. Tissues: normal muscle at uterine cancer stage 1 (1), normal uterine muscle (2), normal uterine muscle at necrotic myoma (3), normal uterine muscle at CC (4), myoma (5), fibromyoma (6), myoma at endometrial cancer (7), and fibromyoma (8). (D) Immunoblot of TrpRS from bovine pancreas (BP): purified TrpRS (7 μg) or postmitochondrial extract (50 μg). Note that ^{32}P-TrpRS was undetectable in BP postmitochondrial extracts under experimental conditions (A). Blots developed with 4-Cl-1-naphthol (B) or DAB (C, D). Positions of TrpRS (arrows), serum albumin (SA), and protein markers (numbers) are also indicated.

Mechanisms of tryptamine activity in connection with TrpRS. Tryptamine binds protein sulfhydryl groups but not disulfide bonds in rat brain synaptic membranes [53]. *N*-ethylmaleimide modifies cysteine residues and inhibits tryptamine binding to membrane proteins. TrpRS is associated with plasma, mitochondrial, and vesicle membranes [24]. On reaction with *N*-ethylmaleimide, the enzymatically active dimeric bTrpRS dissociates into inactive monomeric subunits. The monomeric structure is stabilized by the blocking of the –SH groups exposed during the dissociation with a half-life of dissociation ~30 minutes [54]. The *N*-ethylmaleimide–treated dissociated TrpRS subunits were aggregated [54]. The TrpRS peptide carrying the –SH group was located near the binding site of tryptophan [55]. The enzyme at a concentration higher than 10 to 15 μM (~1 mg/ml) underwent polymerization and aggregation [44]. There is no direct evidence indicating that tryptamine binds or modifies sulfhydryl groups in TrpRS. Structural data clearly show that the mini-hTrpRS N-terminal β-hairpin (residues 83-93) is defined in the tryptophanamide (tryptophan analog)-ATP–bound complex and partially defined in the tryptophan-AMP–bound complex but disordered in the Trp-bound complex and in the free mini-TrpRS [56]. The tryptophanamide-stimulated transition from the disordered state into the β-hairpin conformation may be implicated in the TrpRS fibril formation and aggregation [23,24]. The *E. coli* TrpRS is able to form tryptophanamide [57]. The K_i of tryptophanamide, which is a competitive inhibitor of *Bacillus stearothermophilus* TrpRS with respect to tryptophan, was measured to be 2.5×10^{-6} M. Tryptophanamide (Figure W6), therefore, has a higher affinity for the synthetase than the substrate tryptophan [58]. The structural data on tryptamine-TrpRS or tryptophanol-TrpRS complexes are not available. Tryptamine binds to tryptophan binding site in dimeric TrpRS, inactivates TrpRS, and mediates its aggregation *in vivo*. In addition, the x-ray crystallographic structural analysis of tryptamine complexes with 3-methylcytosine and 7-methylguanine revealed the prominent stacking interactions of tryptamine with the methylated nucleic acid bases [59]. The biologic implication of these interactions can be significant in connection with diminished capacity of DNA from human and hamster cell sublines to bind the hTrpRS gene–specific

probes in Southern blot DNA-DNA hybridization after the prolonged tryptamine treatment [21]. The high amounts of steadily accumulated tryptamine are not required to cause the cell death and TrpRS aggregation. On the contrary, the rapid protein turnover with a half-life of different proteins ranging from a few minutes to hours supports a hit-and-run mechanism for tryptamine cytotoxicity.

Equilibrium of TrpRS Phosphorylation, Expression, and Enzymatic Activity in Normal and Tumor Human Tissues

Endogenous TrpRS is analyzed in postsurgical tissue samples (n = 18). After *in vitro* phosphorylation with [γ-^{32}P]ATP, ^{32}P-TrpRS was detected in tissue samples of human OVC (2 cases) and CC epithelium but was not undetected in corpus uterine cancer, myomas, normal placenta, and liver by immunoprecipitation with monospecific anti-TrpRS antibodies (Figure 7*A*). TrpRS is phosphorylated in human tissue extracts in a Mg^{2+}-dependent mode. These data correlate with immunoblot analysis demonstrating TrpRS increase in OVC and decrease in myomas compared with normal human tissues (Figure 7, *B* and *C*). Assay of enzymatic TrpRS activity in tryptophan-dependent ATP-[^{32}P]PP_i exchange demonstrated the highest activity in both OVC cases of five tested tissues (Table W7). Tryptophan-dependent ATP-PP_i exchange in OVC tissue extracts was two to three times higher than in normal human placenta and liver. The lowest activity was detected in uterine cancer (5.3 times lower than in placenta). The control samples contained normal bovine liver (Figure 7*B*, *lane 19*), bovine pancreatic tissue extract, and bovine purified bTrpRS (Figure 7*D*). In a previous study, anti-TrpRS IgG antibodies were detected in serum of patient with OVC [38]. In this study, serum of CC stimulated TrpRS phosphorylation (T5, Figures 1 and 4) and did not contain histone-specific PK (T5, Figure 5). OVC serum did not contain histone-specific PK similar to other cancer sera (Figure 5*E*). These data demonstrate that the level of hTrpRS phosphorylation correlate with TrpRS enzymatic activity and protein expression at least in OVC and normal tissues.

References

[1] Ghanipour A, Jirstrom K, Ponten F, Glimelius B, Pahlman L, and Birgisson H (2009). The prognostic significance of tryptophanyl-tRNA synthetase in colorectal cancer. *Cancer Epidemiol Biomarkers Prev* **18**, 2949–2956.

[2] Arnouk H, Merkley MA, Podolsky RH, Stoppler H, Santos C, Alvarez M, Mariategui J, Ferris D, Lee JR, and Dynan WS (2009). Characterization of molecular markers indicative of cervical cancer progression. *Proteomics Clin Appl* **3**, 516–527.

[3] Paley EL, Paley DE, Merkulova-Rainon T, and Subbarayan PR (2011). Hypoxia signature of splice forms of tryptophanyl-tRNA synthetase marks pancreatic cancer cells with distinct metastatic abilities. *Pancreas* **40**, 1043–1056.

[4] Morita A, Miyagi E, Yasumitsu H, Kawasaki H, Hirano H, and Hirahara F (2006). Proteomic search for potential diagnostic markers and therapeutic targets for ovarian clear cell adenocarcinoma. *Proteomics* **6**, 5880–5890.

[5] Terasaka S, Aita Y, Inoue A, Hayashi S, Nishigaki M, Aoyagi K, Sasaki H, Wada-Kiyama Y, Sakuma Y, Akaba S, et al. (2004). Using a customized DNA microarray for expression profiling of the estrogen-responsive genes to evaluate estrogen activity among natural estrogens and industrial chemicals. *Environ Health Perspect* **112**, 773–781.

[6] Wieland S, Thimme R, Purcell RH, and Chisari FV (2004). Genomic analysis of the host response to hepatitis B virus infection. *Proc Natl Acad Sci USA* **101**, 6669–6674.

[7] Brinkmann MM, Pietrek M, Dttrich-Breiholz O, Kracht M, and Schulz TF (2007). Modulation of host gene expression by the K15 protein of Kaposi's sarcoma–associated herpesvirus. *J Virol* **81**, 42–58.

[8] Zhu H, Cong JP, Mamtora G, Gingeras T, and Shenk T (1998). Cellular gene expression altered by human cytomegalovirus: global monitoring with oligonucleotide arrays. *Proc Natl Acad Sci USA* **95**, 14470–14475.

[9] Cen S, Javanbakht H, Kim S, Shiba K, Craven R, Rein A, Ewalt K, Schimmel P, Musier-Forsyth K, and Kleiman L (2002). Retrovirus-specific packaging of aminoacyl-tRNA synthetases with cognate primer tRNAs. *J Virol* **76**, 13111–13115.

[10] Mazurenko NN, Kogan EA, Zborovskaya IB, and Kisseljov FL (1992). Expression of pp60c-src in human small cell and non–small cell lung carcinomas. *Eur J Cancer* **28**, 372–377.

[11] Ishizawar R and Parsons SJ (2004). c-Src and cooperating partners in human cancer. *Cancer Cell* **6**, 209–214.

[12] Paley EL (1997). A mammalian tryptophanyl-tRNA synthetase is associated with protein kinase activity. *Eur J Biochem* **244**, 780–788.

[13] Manning G, Whyte DB, Martinez R, Hunter T, and Sudarsanam S (2002). The protein kinase complement of the human genome. *Science* **298**, 1912–1934.

[14] Cynober LA (2004). *Metabolic and Therapeutic Aspects of Amino Acids in Clinical Nutrition*. CRC Press, Boca Raton, FL. pp. 1–755.

[15] Muscaritoli M, Conversano L, Petti MC, Torelli GF, Cascino A, Mecarocci S, Annicchiarico MA, and Rossi FF (1999). Plasma amino acid concentrations in patients with acute myelogenous leukemia. *Nutrition* **15**, 195–199.

[16] Cascino A, Cangiano C, Ceci F, Franchi F, Mineo T, Mulieri M, Muscaritoli M, and Rossi FF (1991). Increased plasma free tryptophan levels in human cancer: a tumor related effect? *Anticancer Res* **11**, 1313–1316.

[17] Laviano A, Cascino A, Muscaritoli M, Fanfarillo F, and Rossi FF (2003). Tumor-induced changes in host metabolism: a possible role for free tryptophan as a marker of neoplastic disease. *Adv Exp Med Biol* **527**, 363–366.

[18] Cascino A, Muscaritoli M, Cangiano C, Conversano L, Laviano A, Ariemma S, Meguid MM, and Rossi FF (1995). Plasma amino acid imbalance in patients with lung and breast cancer. *Anticancer Res* **15**, 507–510.

[19] van Sluijters DA, Dubbelhuis PF, Blommaart EF, and Meijer AJ (2000). Amino-acid–dependent signal transduction. *Biochem J* **351**(Pt 3), 545–550.

[20] Paley EL, Baranov VN, Alexandrova NM, and Kisselev LL (1991). Tryptophanyl-tRNA synthetase in cell lines resistant to tryptophan analogs. *Exp Cell Res* **195**, 66–78.

[21] Paley EL (1999). Tryptamine-mediated stabilization of tryptophanyl-tRNA synthetase in human cervical carcinoma cell line. *Cancer Lett* **137**, 1–7.

[22] Paley EL, Denisova G, Sokolova O, Posternak N, Wang X, and Brownell AL (2007). Tryptamine induces tryptophanyl-tRNA synthetase–mediated neurodegeneration with neurofibrillary tangles in human cell and mouse models. *Neuromolecular Med* **9**, 55–82.

[23] Paley EL, Smelyanski L, Malinovskii V, Subbarayan PR, Berdichevsky Y, Posternak N, Gershoni JM, Sokolova O, and Denisova G (2007). Mapping and molecular characterization of novel monoclonal antibodies to conformational epitopes on NH_2 and COOH termini of mammalian tryptophanyl-tRNA synthetase reveal link of the epitopes to aggregation and Alzheimer's disease. *Mol Immunol* **44**, 541–557.

[24] Paley EL (2011). Tryptamine-induced tryptophanyl-tRNA^{trp} deficiency in neurodifferentiation and neurodegeneration interplay: progenitor activation with neurite growth terminated in Alzheimer's disease neuronal vesicularization and fragmentation. *J Alzheimers Dis* **26**, 263–298.

[25] Rahman-Roblick R, Roblick UJ, Hellman U, Conrotto P, Liu T, Becker S, Hirschberg D, Jornvall H, Auer G, and Wiman KG (2007). p53 targets identified by protein expression profiling. *Proc Natl Acad Sci USA* **104**, 5401–5406.

[26] Rapaport E, Zamecnik PC, and Baril EF (1981). HeLa cell DNA polymerase alpha is tightly associated with tryptophanyl-tRNA synthetase and diadenosine 5′,5‴-P1,P4-tetraphosphate binding activities. *Proc Natl Acad Sci USA* **78**, 838–842.

[27] Wakasugi K (2007). Human tryptophanyl-tRNA synthetase binds with heme to enhance its aminoacylation activity. *Biochemistry* **46**, 11291–11298.

[28] Croce AC, Santamaria G, De SU, Lucchini F, Freitas I, and Bottiroli G (2011). Naturally-occurring porphyrins in a spontaneous-tumour bearing mouse model. *Photochem Photobiol Sci* **10**, 1189–1195.

[29] Venema RC and Traugh JA (1991). Protein kinase C phosphorylates glutamyl-tRNA synthetase in rabbit reticulocytes stimulated by tumor promoting phorbol esters. *J Biol Chem* **266**, 5298–5302.

[30] Aoki T, Yamada N, Tomita I, Kako Y, and Imamura T (1987). Caseins are cross-linked through their ester phosphate groups by colloidal calcium phosphate. *Biochim Biophys Acta* **911**, 238–243.

[31] Desai PR, Ujjainwala LH, Carlstedt SC, and Springer GF (1995). Anti–Thomsen-Friedenreich (T) antibody-based ELISA and its application to human breast carcinoma detection. *J Immunol Methods* **188**, 175–185.

[32] Kellermann O, Tonetti H, Brevet A, Mirande M, Pailliez JP, and Waller JP (1982). Macromolecular complexes from sheep and rabbit containing seven

aminoacyl-tRNA synthetases. I. Species specificity of the polypeptide composition. *J Biol Chem* **257**, 11041–11048.

[33] Paley EL (1996). Phosphorylation of T antigen and p53 in carcinogen-treated SV40-transformed Chinese hamster cells. *Carcinogenesis* **17**, 939–945.

[34] Lam KS and Kasper CB (1980). Selective endogenous phosphorylation of two liver microsomal polypeptides in the presence of micromolar levels of Mg^{2+} ion. *J Biol Chem* **255**, 259–266.

[35] Wakasugi K (2010). An exposed cysteine residue of human angiostatic mini tryptophanyl-tRNA synthetase. *Biochemistry* **49**, 3156–3160.

[36] Gnad F, Gunawardena J, and Mann M (2011). PHOSIDA 2011: the posttranslational modification database. *Nucleic Acids Res* **39**, D253–D260.

[37] Scheinker VS, Beresten SF, Mazo AM, Ambartsumyan NS, Rokhlin OV, Favorova OO, and Kisselev LL (1979). Immunochemical studies of beef pancreas tryptophanyl-tRNA synthetase and its fragments. Determination of the number of antigenic determinants and a comparison with tryptophanyl-tRNA synthetases from other sources and with reverse transcriptase from avian myeloblastosis virus. *Eur J Biochem* **97**, 529–540.

[38] Paley EL, Alexandrova N, and Smelansky L (1995). Tryptophanyl-tRNA synthetase as a human autoantigen. *Immunol Lett* **48**, 201–207.

[39] Raught B, Gingras AC, Gygi SP, Imataka H, Morino S, Gradi A, Aebersold R, and Sonenberg N (2000). Serum-stimulated, rapamycin-sensitive phosphorylation sites in the eukaryotic translation initiation factor 4GI. *EMBO J* **19**, 434–444.

[40] Bhattacharyya J and Das KP (1999). Molecular chaperone-like properties of an unfolded protein, alpha(s)-casein. *J Biol Chem* **274**, 15505–15509.

[41] Sakono M, Motomura K, Maruyama T, Kamiya N, and Goto M (2011). Alpha casein micelles show not only molecular chaperone-like aggregation inhibition properties but also protein refolding activity from the denatured state. *Biochem Biophys Res Commun* **404**, 494–497.

[42] Eilen E and Krakow JS (1977). Cyclic AMP–mediated intersubunit disulfide crosslinking of the cyclic AMP receptor protein of *Escherichia coli*. *J Mol Biol* **114**, 47–60.

[43] Martinez M, Fernandez E, Frank A, Guaza C, de la Fuente M, and Hernanz A (1999). Increased cerebrospinal fluid cAMP levels in Alzheimer's disease. *Brain Res* **846**, 265–267.

[44] Iborra F, Dorizzi M, and Labouesse J (1973). Tryptophanyl-transfer ribonucleic-acid synthetase from beef pancreas. Ligand binding and dissociation equilibrium between the active dimeric and inactive monomeric structures. *Eur J Biochem* **39**, 275–282.

[45] Kovaleva GK, Zheltova AO, Nikitushkina TV, Egorov TA, Musoljamov AC, and Kisselev LL (1992). Carbohydrates in mammalian tryptophanyl-tRNA synthetase. *FEBS Lett* **309**, 337–339.

[46] Roussel RR, Brodeur SR, Shalloway D, and Laudano AP (1991). Selective binding of activated pp60c-src by an immobilized synthetic phosphopeptide modeled on the carboxyl terminus of pp60c-src. *Proc Natl Acad Sci USA* **88**, 10696–10700.

[47] Pendergast AM, Venema RC, and Traugh JA (1987). Regulation of phosphorylation of aminoacyl-tRNA synthetases in the high molecular weight core complex in reticulocytes. *J Biol Chem* **262**, 5939–5942.

[48] Arif A, Jia J, Moodt RA, DiCorleto PE, and Fox PL (2011). Phosphorylation of glutamyl-prolyl tRNA synthetase by cyclin-dependent kinase 5 dictates transcript-selective translational control. *Proc Natl Acad Sci USA* **108**, 1415–1420.

[49] Dubbelhuis PF and Meijer AJ (2002). Hepatic amino acid–dependent signaling is under the control of AMP-dependent protein kinase. *FEBS Lett* **521**, 39–42.

[50] Domino EF and Gahagan S (1977). *In vitro* half-life of 14-C-tryptamine in whole blood of drug-free chronic schizophrenic patients. *Am J Psychiatry* **134**, 1280–1282.

[51] Ramos AJ, Tagliaferro P, Saavedra JP, and Brusco A (1999). Tryptamine, serotonin and catecholamines: an immunocytochemical study in the central nervous system. *Int J Neurosci* **99**, 123–137.

[52] Roe CM, Fitzpatrick AL, Xiong C, Sieh W, Kuller L, Miller JP, Williams MM, Kopan R, Behrens MI, and Morris JC (2010). Cancer linked to Alzheimer disease but not vascular dementia. *Neurology* **74**, 106–112.

[53] Serikyaku S, Saito M, and Ishitani R (1990). Effects of protein-modifying reagents on brain tryptamine binding sites: possible involvement of a thiol group in temperature-induced high-affinity [^{3}H]tryptamine binding sites. *Jpn J Pharmacol* **52**, 51–57.

[54] Iborra F, Labouesse B, and Labouesse J (1975). Structure-activity relationships in tryptophanyl transfer ribonucleic acid synthetase from beef pancreas. Influence of the alkylation of the sulfhydryl groups on the dimer-monomer equilibrium. *J Biol Chem* **250**, 6659–6665.

[55] Iborra F, Gros C, Labouesse B, and Labouesse J (1975). Molecular aspects of the inactivation of tryptophanyl transfer ribonucleic acid synthetase by *N*-ethylmaleimide. *J Biol Chem* **250**, 6666–6671.

[56] Shen N, Zhou M, Yang B, Yu Y, Dong X, and Ding J (2008). Catalytic mechanism of the tryptophan activation reaction revealed by crystal structures of human tryptophanyl-tRNA synthetase in different enzymatic states. *Nucleic Acids Res* **36**, 1288–1299.

[57] Andrews D, Trezeguet V, Merle M, Graves PV, Muench KH, and Labouesse B (1985). Tryptophanamide formation by *Escherichia coli* tryptophanyl-tRNA synthetase. *Eur J Biochem* **146**, 201–209.

[58] McArdell JE, Atkinson T, and Bruton CJ (1982). The interaction of tryptophanyl-tRNA synthetase with the triazine dye Brown MX-5BR. *Eur J Biochem* **125**, 361–366.

[59] Ishida T, Ueda H, Segawa K, Doi M, and Inoue M (1990). Prominent stacking interaction with aromatic amino acid by *N*-quarternization of nucleic acid base: x-ray crystallographic characteristics and biological implications. *Arch Biochem Biophys* **278**, 217–227.

Table W1. TrpRS Phosphorylation Tested with Blood Sera of Healthy Individuals and Cancer Patients.

No. Noncancer Individuals	No. Cancer Patients
15	13

Table W2. Site and Stage of Cancer Tested for Serum-Inducible TrpRS Phosphorylation.

Code	Site	Stage
T1	Stomach cancer	Multiple metastasis
T2	Fast-growing chondroma	n/a
T3	Testicular seminoma	3
T4	Lung cancer	3
T5	CC	3
T6	Bladder cancer	3
T7	Lung cancer	4, metastasis
LPM	CRC	4
L	Leukemia	n/a
T8	Lung cancer, squamous cell carcinoma	4
T9	Recurrent bladder cancer	3
T10	Stomach cancer	n/a
T11	Stomach cancer	4

n/a indicates not applicable.

Table W3. TrpRS and Histones in Serum-Inducible Phosphorylation: Follow-up Study.

Diagnosis at Follow-up, y	Follow-up, y	Diagnosis at Testing	TrpRS Phosphorylation	Histones Phosphorylation
(A) Cancer diagnosed years after testing				
(1) Acute leukemia (deceased)	6	Uterine cancer 8-y after treatment Disease free	High	Low
(2) PC (deceased)	17	GBD	High	$H2B^{+}H4^{+}$
(3) CRC (deceased, 19 y)	15	None	High	Low
(B) Good prognosis for survival				
(4) Disease free	20	CRC	Normal	Low
(C) Suspected, undiagnosed				
(5) Prolapsed uterus, hysterectomy-ovariectomy 19; papillomatosis; kidney cyst; leukocytes, urine (500×10^9/l)	20	Papilloma	High	Normal

Car accident, broken ribs–related hospitalization before acute leukemia was diagnosed in case 1, gallbladder removal (stones) before PC was diagnosed in case 2, and gallbladder removal before CRC was diagnosed in case 4.

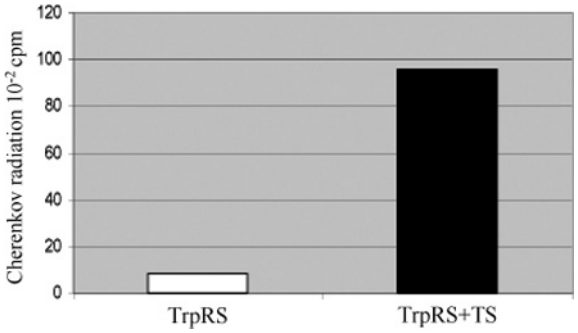

Figure W1. Counting of Cherenkov radiation (~60-kDa bTrpRS): anti-TrpRS serum-inducible TrpRS phosphorylation (TS1, 2 μl). PK assay probe (20 μl) contained 20 μg of bTrpRS, 0.5 μM [γ-^{32}P]ATP (2000 Ci/mmol, 500 μCi/50 μl), and 50 mM 2-ME and incubated for 15 minutes at 37°C. Bands were excised from the gel (12.5% SDS-PAGE); see Figure 2*A* (no cAMP).

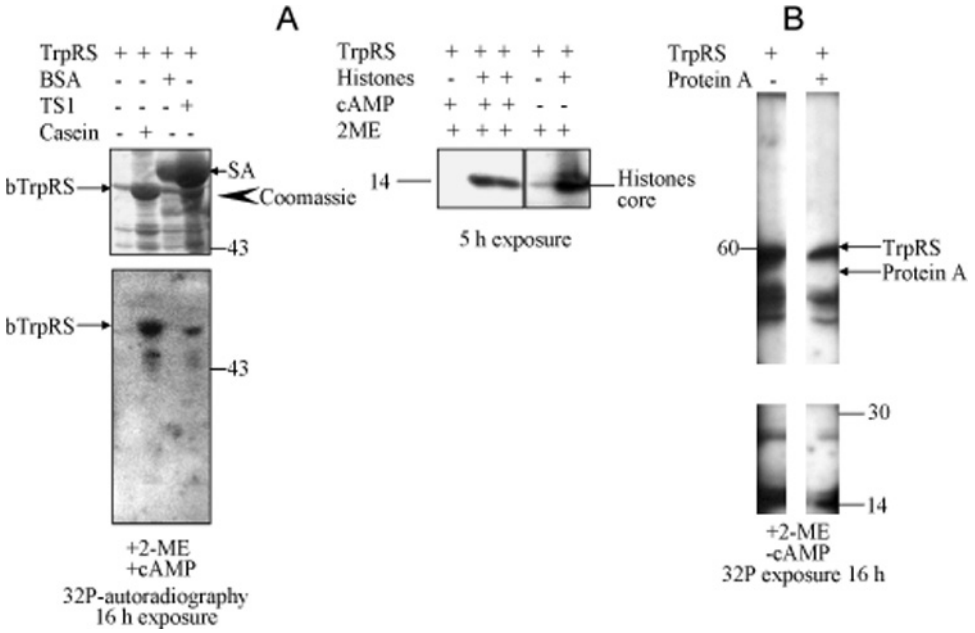

Figure W2. Casein and anti-TrpRS serum but not BSA, histones (A) or protein A (B), work as chaperons for TrpRS in the presence of 2-ME. TrpRS phosphorylated in PK buffer (50 mM 2-ME, 1 mM 5′AMP, 2 mM $MnCl_2$, 5 mM $MgCl_2$, 50 μM EDTA, 3 mM PMSF, 20 mM Tris-HCl, pH 7.5, 1.5 μl of [γ-^{32}P]ATP, 2000 Ci/mmol, 10 μCi/μl) with or without cAMP (100 μM), casein (20 μg), anti-TrpRS serum (TS1, 2 μl), BSA (20 μg), histones (20 μg each, two different extractions), and protein A (20 μg, purified by affinity chromatography; Pasteur Institute of Epidemiology and Microbiology, St. Petersburg, Russia). Positions of rabbit serum albumin (SA) and protein markers (kDa) are shown.

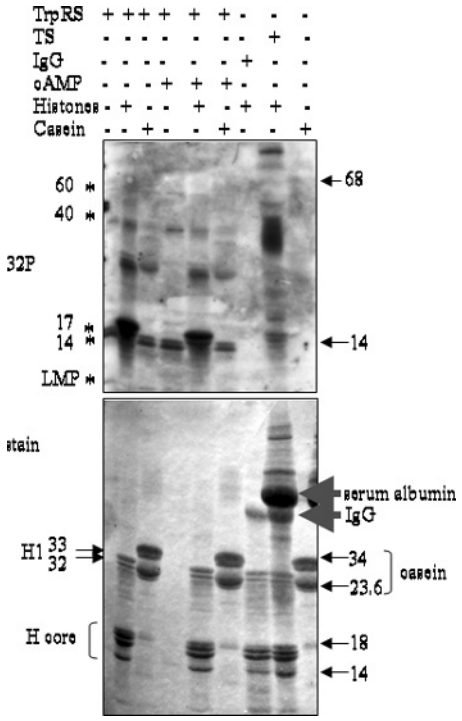

Figure W3. Casein and cAMP independence of TrpRS-PK activity in absence of 2-ME. Incubation was in PK buffer (20 mM Tris-HCl, pH 7.2, 2.5 mM $MgCl_2$, 4 mM $MnCl_2$, 3 mM DFP, [γ-^{32}P]ATP) with or without histones (20 μg), casein (40 μg), TrpRS (10 μg), anti-TrpRS IgG (IgG, 2 μl), anti-TrpRS rabbit serum (TS, 2 μl), and cAMP (100 μM). Lower panel, Coomassie staining (stain); upper panel, autoradiography (^{32}P), x-ray film exposure for 40 hours. The molecular weights of proteins (15% SDS-PAGE) are indicated with arrows. ^{32}P-TrpRS forms are indicated by asterisks (60, 40, 17, and 14 kDa and low–molecular weight peptide [LMP]). Note that casein refolding and cAMP-inhibitory effects are undetectable.

Table W4. Histone-Specific PK in Noncancer and Cancer Sera.

No. Noncancer Individuals	No. Cancer Patients
1. TrpRS tested	
13	13
2. TrpRS nontested	
17	31

Table W5. Diagnosis of Noncancer Individuals Tested for Histone Phosphorylation.

Diagnosis	No. Individual	TrpRS Test
GBD	1	Increase
After acute meningitis	1	Decrease
Papilloma	1	Increase
Psoriasis	3	ND
Pneumonia	10	ND
Myocardial infarction	3	ND
Stomach ulcer	1	ND

ND indicates not determined.

Table W6. Sites of Cancer Cases Tested for Histone-Specific Serum PK.

Site	No. Individuals
Soft tissue sarcoma	2
Brain tumor	1
Breast cancer	1
CC	2
Bladder cancer	3
Lung cancer	2
Osteosarcoma	1
Seminoma	1
Prostate cancer	1
Esophageal cancer	1
OVC	1
CRC	2
Stomach cancer	1
Cancer of unknown primary location	12

Serum-inducible TrpRS phosphorylation has not been tested for these cases.

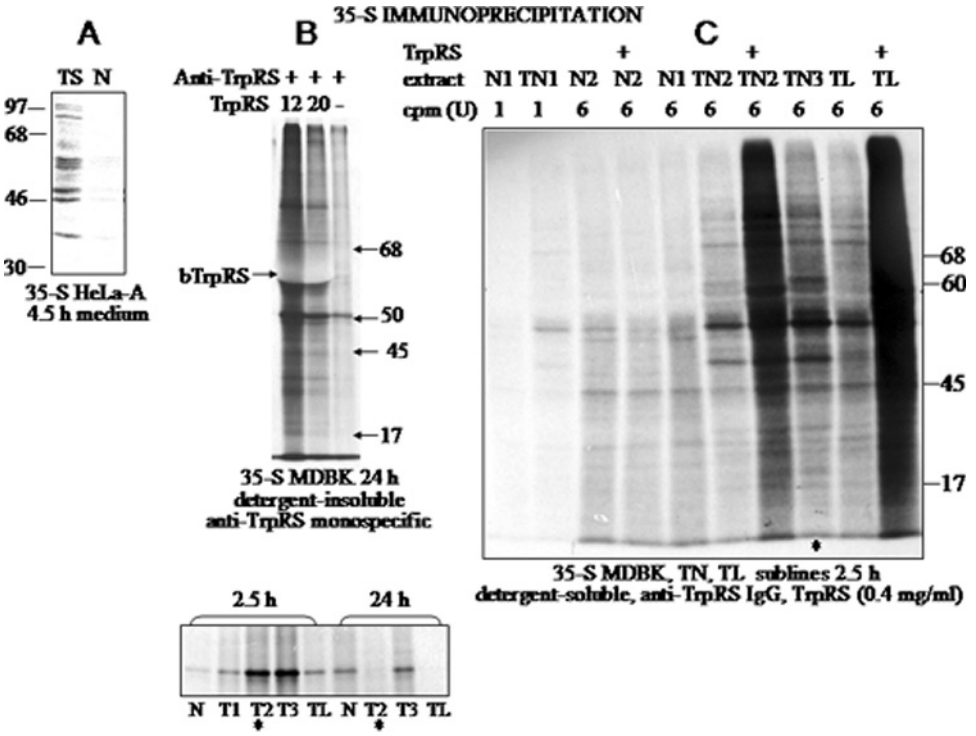

Figure W4. TrpRS immunoprecipitation after *in vivo* labeling with [^{35}S]methionine. TrpRS was immunoprecipitated from [^{35}S]methionine culture medium (250 μl) of tryptamine-resistant human HeLa-A subline [21] (A) or control and treated MDBK cells (B, C). Immunoprecipitation was performed with anti-TrpRS rabbit serum (TS, 10 μl), nonimmune rabbit serum (N, 10 μl), monospecific anti-TrpRS polyclonal antibodies (4.5 μg/probe; B) or anti-TrpRS IgG (40 μg/probe; C). Labeling was during 4.5 hours (A), 2.5 and 24 hours (B), and 2.5 hours (C). Extracts were insoluble in 0.5% Triton X-100 for 15 minutes at 0°C (B) and detergent-soluble (C) extracts (1% NP-40, 10 mM Tris-HCl, pH 7.5, 50 mM KCl, 0.1 mM DTT, 20% glycerol) were examined with anti-TrpRS antibodies or antibodies preincubated with unlabeled purified bTrpRS (12 or 20 μg/300 μl; B, upper) or at 0.4 mg/ml (C) overnight (4°C). In B, ^{35}S-labeled extracts contain 2×10^6 cpm; in C, 7×10^4 cpm (1) or 4.5×10^5 cpm (6) before immunoprecipitation.

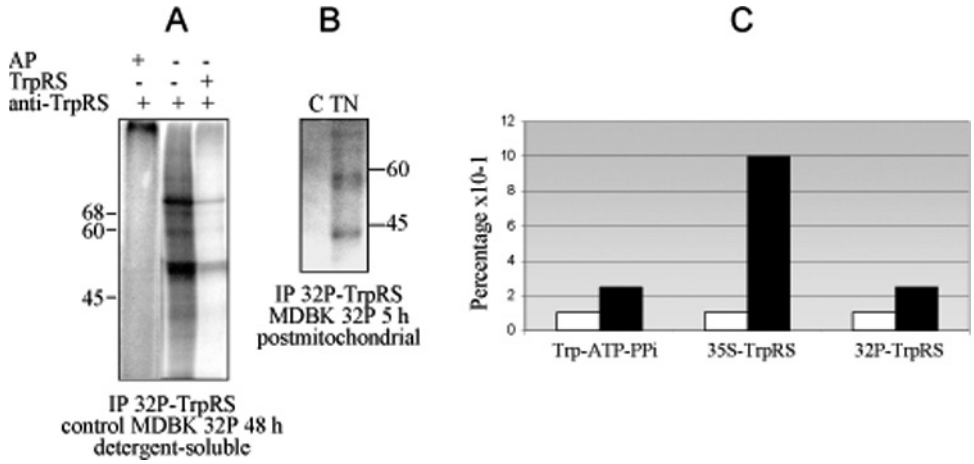

Figure W5. TrpRS equilibrium (tryptophan-dependent ATP-[^{32}P]PP$_i$ exchange and ^{35}S and ^{32}P immunoprecipitation) in control MDBK (white columns) and tryptamine-treated subline TN3/T2 (black columns). (A and B) *In vivo* cell labeling with [^{32}P]orthophosphoric acid (54 mCi/200 μl, 185 pBq/mol). Immunoprecipitation of 1% NP-40–soluble (A) and postmitochondrial (B) extracts with anti-TrpRS polyclonal serum (A) and monospecific anti-TrpRS antibodies (B). Equal ^{32}P-radioactivity (48 hours of labeling) was incubated with anti-TrpRS serum (10 μl) or preincubated anti-TrpRS serum (10 μl + unlabeled TrpRS, 50 μg). Control MDBK cell extract (AP) was treated with *E. coli* alkaline phosphatase (Wartington; 4 U/200 μl of cell lysate) and then with anti-TrpRS antibodies. Postmitochondrial extracts from control (C) and tryptamine-treated (TN) MDBK cells obtained by homogenization (Dounce glass/glass homogenizer) in 0.25 M sucrose, 0.01 M Tris-HCl pH 7.5, 1 mM EDTA, and 3 mM DFP after 5 hours of labeling. Extracts (150 μl, 1.5 $\times$ 10^7 cpm) were incubated with monospecific anti-TrpRS antibodies (15 μg) for 3 hours at 25°C (B). TrpRS was not detectably phosphorylated in postmitochondrial fraction of control cells. (C) For TrpRS-catalyzed tryptophan-dependent ATP-PP$_i$ exchange, cells were extracted in 0.1% Triton X-100, 50 mM NaCl, 2 mM $MgCl_2$, 10 mM 2-ME, 50 mM Tris-HCl pH 7.5, and 2 mM DFP for 30 minutes at 0°C. To remove endogenous tryptophan, detergent-soluble fractions (500 μl) were dialyzed against 2 L (two changes) of buffer (50 mM NaCl, 10 mM 2-ME, 10 mM Tris-HCl pH 7.5) for 24 hours at 4°C. Protein concentration was measured in extracts using Bradford reagent. Enzymatic reaction (200 μl) in the presence of Tris-HCl pH 7.5, Mg^{2+}, 0.2% dialyzed gelatin, ATP, PP$_i$, and [^{32}P]PP$_i$ was conducted (37°C) as described previously [20]. Concentrations of tryptophan (0-1 μM) and cell extracts (25-50 μg/10-20 μl) and incubation time (3-30 min) varied for the reaction optimization. Immunoprecipitation of detergent-soluble (1% NP-40) fractions with anti-TrpRS IgG was performed after 2.5 hours of labeling (^{35}S and ^{32}P). Each of these experiments was repeated at least three times, and representative results are shown.

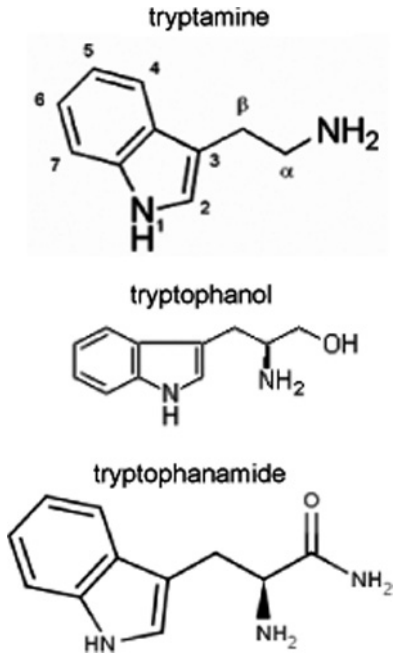

Figure W6. Molecular structures of TrpRS inhibitors, tryptophanamide, tryptamine, and tryptophanol.

Table W7. TrpRS Catalyzed Tryptophan-Dependent ATP-[^{32}P]PP$_i$ Exchange in Postmitochondrial Human Tissue Extracts.

Human Tissue Extract	Tryptophan-Dependent ATP-[^{32}P]PP$_i$ Exchange (cpm)
Placenta	940
Liver (hepatitis)	810
Uterine cancer	175
OVC I	2710
OVC II	1860

Shown are representative results from an experiment that was repeated at least three times. Counts (cpm) for control probes incubated without tryptophan were deducted.